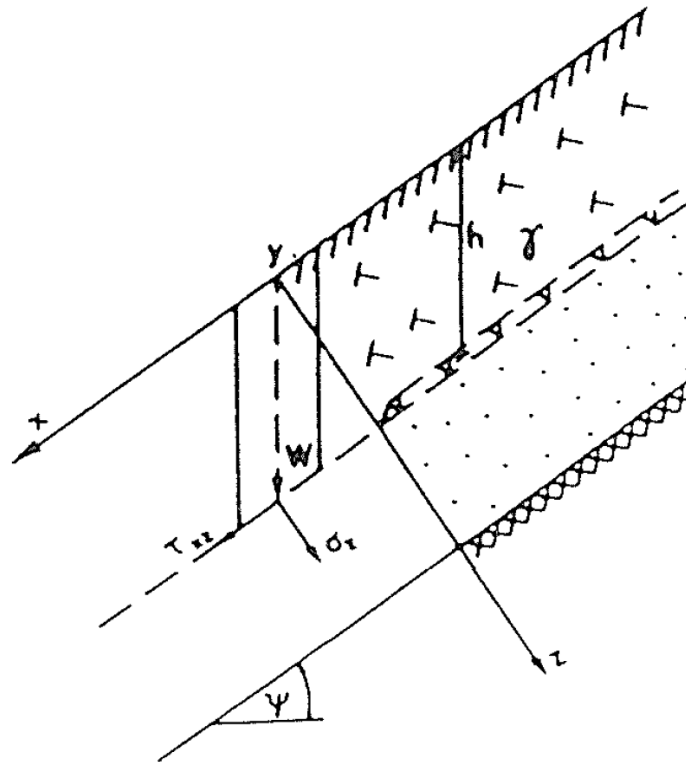


Skier stability index

- An additional tool for snow avalanche forecasting in Norway?



Master Thesis in Meteorology

Elise Gloppen Hunnes

June 2018



UNIVERSITY OF BERGEN
Faculty of Mathematics and Natural Sciences

Front figure - Coordinate system used in calculating the stability index (S) from Föhn (1987)

Abstract

With more people running to the mountains for skiing backcountry terrain, the need for a good snow avalanche forecast is dire. Today's forecast is based on the weather forecast, snow observations by professional observers and modeled snow data. This thesis will investigate if a stability index can contribute to the current avalanche forecast. Three variations of Skier stability index (S') has been calculated for the 21 A-regions used in avalanche forecasting in Norway. The calculations have been done using three different griddings; full region, deployment areas and point of avalanche. Data sets used are snow data from The Norwegian Water Resources and Energy Directorate (NVE) and meteorological data from MetCoOp Ensemble Prediction System (MEPS) for the avalanche forecasting seasons from 2014-2017 (1st December- 31st May). Success rates of S' on days where avalanches have been reported were checked to investigate the potential of the index. Versions 1 and 2 (assuming no weak layers in the snowpack) showed low success rate, with highest average of 34 % semi-success ($1 < S' \leq 1.5$). Version 3 (assuming buried surface hoar layer) showed a high success rate (80 %), but also gives false positive on days with no observed avalanches. At present time the index does not contribute to the avalanche forecast because of the low success rates. Further investigations in modified ways of using the skier stability index can still be interesting. With an improved avalanche observation record for the latest season (2018), validation of avalanche research will become more reliable.

Acknowledgments

First of all I want to thank my supervisor Asgeir Sorteberg, for giving me the opportunity to dig deeper into a field I find so interesting. Thank you for great matlab help when needed, for good guidance along the way, and for letting me find my own path in my research.

I would also like to thank Mari Hunnes, for always having time to listen to all my triumphs and frustrations along the way. Thank you for good help in proof reading, even with some more interesting corrections (ref: the radioactive processes of the snow). Big gratitude also goes to Eivind Kolås, for providing the latex template, and to Katrine Hiort, for always listening to my questions, even if they didn't always make sense.

The five years through this study would not have been the same without all my fellow students. Thank you for all coffee breaks, volleyball breaks, break dance - dance offs, off-railing high five discussions, and the hardcore study sessions in-between.

Contents

Contents	i
List of Figures	ii
List of Tables	iii
Abbreviations	iv
Symbols	v
1 Introduction	1
1.1 Motivation	1
1.2 Research design	3
1.3 Outline	4
2 Background	5
2.1 Snow physics	5
2.1.1 Snow formation	5
2.1.2 Snow microstructure	6
2.2 Introduction to snow avalanches	7
2.3 Dry slab avalanches	7
2.3.1 Terrain	8
2.3.2 Snowpack	8
2.3.3 Critical balance	10
2.3.4 Triggers	12
2.4 Avalanche forecasting in Norway	13
3 Data and method	16
3.1 Data	16
3.1.1 Snow cover data	16
3.1.2 Meteorological data	17
3.1.3 Avalanche history record	18
3.2 Area of interest/focus	19

3.2.1	Forecast regions	19
3.2.2	Avalanche deployment areas	19
3.3	Method	22
3.3.1	Stability index S	22
3.3.2	Skier stability index S'	24
3.3.3	Surface hoar formation from latent heat flux	25
3.3.4	Descriptitve statistics	26
4	Results	28
4.1	Sensitivity Analysis	28
4.1.1	Sensitivity analysis of Skier Stability Index	28
4.1.2	Sensitivity analysis of Q_E	29
4.2	Surface hoar growth	31
4.3	Skier Stability Index (S')	32
5	Discussion	45
5.1	Interpretation of results	45
5.1.1	Surface hoar growth	45
5.1.2	V1 vs V2 vs V3	46
5.1.3	Deployment areas vs Region vs Point of avalanche	46
5.2	Limitations	47
5.2.1	Skier stability index	47
5.2.2	Avalanche history record	47
5.2.3	Spatial and temporal resolution of the data	48
6	Summary and outlook	50
6.1	Summary	50
6.2	Recommendation for further work	51
7	Bibliography	52
	APPENDICES	54
A	Weak layers and interfaces in the snowpack	55

List of Figures

1.1	Avalanche accidents from 2008 by season	1
1.2	Avalanche accidents from 2014 by category	2
1.3	Avalanche forecast 'as is' vs with skier stability index	3
2.1	Slab avalanche vs point release avalanche	7
2.2	Three layered snowpack	9
2.3	Surface hoar creation	9
2.4	Shear forces acting on a slope.	10
2.5	Object under shear stress.	11
2.6	Stability tests in field; Rutschblock and Compression test	12
2.7	Varsom.no	13
2.8	RegObs	13
2.9	Varsom.no avalanche forecast	14
2.10	Avalanche danger scale	15
3.1	Distribution of snow avalanches recorded by attribute	18
3.2	Location of observed avalanches for winter seasons 2014 - 2017	19
3.3	Map of avalanche regions	21
3.4	Snow avalanche deployment area	22
3.5	Slab avalanche coordinate system (Föhn, 1987)	23
3.6	Slab cross section with peak stress induced by static skier	25
4.1	Skier stability index (S') sensitivity analysis	29
4.2	Latent heat flux (Q_E) sensitivity analysis	30
4.3	Time series of MEPS weather data, Q_E and surface hoar size	31
4.4	Precipitation and surface hoar vs observed avalanches	32
4.5	Skier stability index, all runs, Voss 2014-2017	34
4.6	Skier stability index, all runs, Lyngen 2014-2017	35
4.7	Boxplot skier stability index, Voss winter season 2014	36
4.8	Skier stability index (S'), Voss 16th March 2014, with distribution.	37
4.9	Success rate for skier stability index, full region, v2	38

4.10	Success rate for skier stability index, full region, v1	39
4.11	Success rate for skier stability index, full region, v3	40
4.12	Skier stability index (S'), v2, in points of observed avalanches, Lyngen 2014	41
4.13	Skier stability index (S'), v2, in points of observed avalanches, Voss 2014	42
4.14	Success rate skier stability index v2 point	43
4.15	Success rate skier stability index v1 point	44

List of Tables

2.1	ICSI nine newly fallen snow classification	6
2.2	Slope incline guidelines by McClung (2006)	8
3.1	Variables used from NVE	16
3.2	Variables used from MEPS	17
3.3	Snow avalanche observations attributes	18
3.4	Avalanche forecasting regions	20
3.5	Strength-density regression by grain form by Jamieson and Johnston (2001)	24
3.6	Skier stability index (S') version descriptions	25
4.1	Latent heat flux sensitivity analysis results	30
A.1	Weak layers and interfaces in the snowpack	56

Abbreviations

CT	column test
ECT	extended column test
ICSI	International Commission on Snow and Ice
JBV	Norwegian National Rail Administration
MEPS	MetCoOp Ensemble Prediction System
MET-Norway	Meteorological Institute of Norway
NGI	Norwegian Geotechnical Institute
NGU	Geological Survey of Norway
NP	nonpersistent layer
NPRA	Norwegian Public Road Administration
NVE	The Norwegian Water Resources and Energy Directorate
P	persistent layer
S	Stability Index
S'	Skier stability index
SWE	snow water equivalent

Symbols

C_e	Bulk transfer coefficient
Q_E	Latent heat flux
T_A	Air temperature
T_S	Surface temperature
$\Delta\tau_{xz}$	Artificially induced stress
Ψ	Inclination of slope
α_{max}	Angle
ϕ	Internal friction
ρ_a	Air density
ρ_{ice}	Ice density 917 kgm^{-3}
ρ	Snow density
σ_{zz}	Normal stress
τ_s	Shear strength of the weakest layer in snowpack
τ_{xz}	Shear stress component parallel to the slope at a given slope location
g	Gravitational constant 9.81 ms^{-2}
h	Slab thickness
l	Length of ski
m	Mass of skier

1 | Introduction

1.1 Motivation

Over the last decade backcountry skiing has become increasingly popular. It is no longer just the 'skibums' strapping skins on their skis to explore the wilder, steeper mountains of Norway. It has now become a popular sport amongst Norwegians. A few go for the guided tours, with knowledgeable tour guides managing the safety and keeping aware of the dangers of the snowpack for them, but most seek to find the untouched powder in remote locations by themselves. Backcountry skiing, or ski touring, does not require a license of any sort, but mother nature can be cruel, and it is best to learn the warning signs before moving into new terrain. A good understanding of the avalanche danger and warning signals can prevent avalanche accidents.

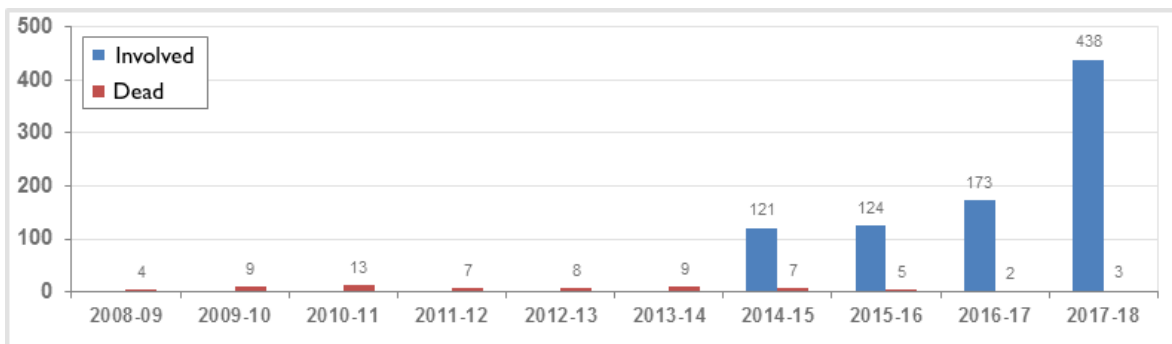


Figure 1.1 – Overview of people involved in snow avalanche accidents from fall 2008. Registering of 'involved' started season 2014-15 and includes both fatalities and survivors. Modified from Varsom.no (2018c).

In Figure 1.1 we can see an overview of how many people have been involved in snow avalanche accidents, either triggering, getting caught, buried or fatalities. The accidents are collected by Norwegian Geotechnical Institute (NGI), The Norwegian Water Resources and Energy Directorate (NVE), Read Cross, Internet search and regobs, and distributed from Varsom.no (2018c). 'Involved' are the number of people present when the avalanche released, and could have been or was taken by the avalanche (also including fatalities). 'Dead' gives the number of these who lost their lives. 'Involved' is only

registered from season 2014-15, while NGI has been registering fatalities since 1992. The numbers of 'Involved' are most likely underestimated, as there is reasons to believe that many near misses are not registered. In Figure 1.2 the avalanche accidents from 2014 are sorted by category. It clearly shows the highest amount of registered snow avalanche accidents happen while skiing (term used loosely for skiing, snowboarding and on-foot activity). With the combination of higher interest in backcountry activities, and an upward trend in accidents, the need for a good avalanche forecasting system is clear.

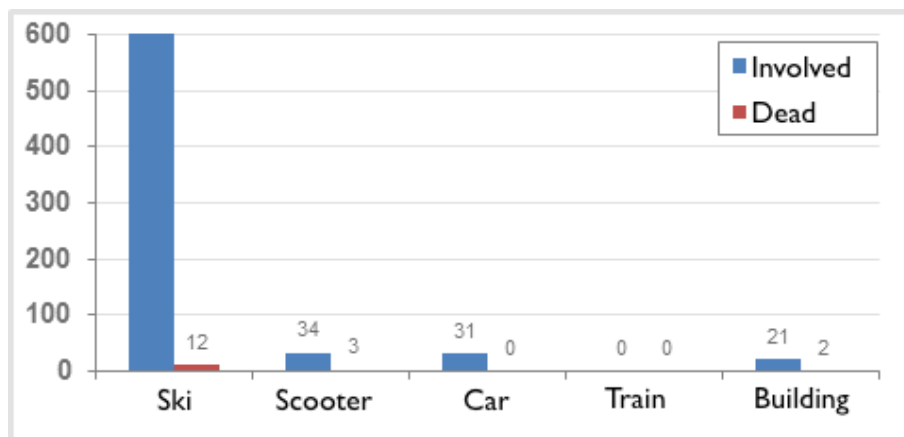


Figure 1.2 – Avalanche danger from 2014 sorted by categories ski (ski, snowboard and on foot), snow scooter and car (all vehicles excluding snow scooters). 'Involved' includes both fatalities and survivors. Modified from Varsom.no (2018c).

Public avalanche forecast was introduced in Norway in January 2013, and has since the winter season of 2013-2014 been producing daily avalanche forecasts for several regions of Norway. The forecast is at present time based on 'now situation'-understanding from weather data, snowpack model and manual observations made by trained snowpack observers in the forecast regions, as seen in Figure 1.3. The now situation is then analyzed with the weather forecast, before an evaluation is done of what avalanche problems and what avalanche danger we can expect. The forecast is highly dependent on manual observations registered either by trained observers, or observations from the public.

An additional factor that could be used is indication of stability in snowpack. Since the earlier work with stability index done by Roch (1966a), there has been several attempts at estimating a stability index for the snow cover. Including stability index derived from shear strength measurements by, amongst other, Conway and Abrahamson (1984) and Landry et al. (2004). As well as skier stability index derived from shear frame measurements, such as Föhn (1987), which is a modified version of stability index by Roch (1966a). The use of this as an addition to the avalanche forecast has not been

done in Norway earlier. The inclusion of stability index in the process, as indicated in Figure 1.3, will then help the forecaster have a new tool to identify potential avalanche problems in the terrain.

Can skier stability index be a contribution to the present avalanche forecast in Norway at present day?

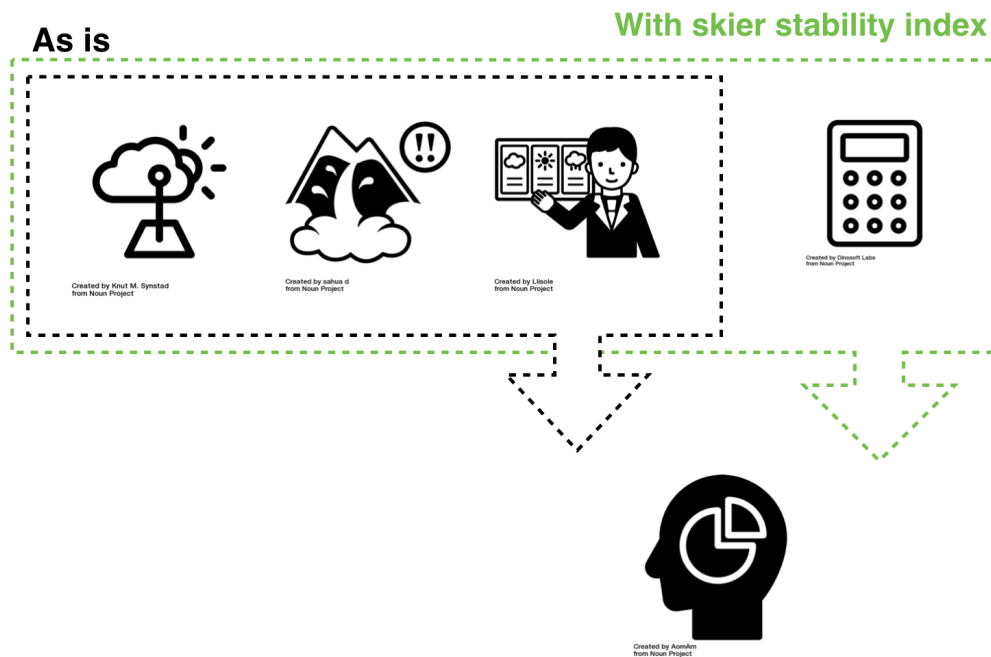


Figure 1.3 – Avalanche forecast 'as is' in black frame. Including weather observations, avalanche and snowpack observations, and the forecast for the coming days, before it is analyzed by avalanche forecaster. Contribution of Skier stability index in the green frame.

1.2 Research design

I will be using modeled snowpack data and meteorological data from winter season (defined as 1st December - 31st May) 2013/2014 - 2016/2017 for the extent of Norway. I will use the skier stability index, which is a modified stability index first introduced by Roch (1966b), later modified by Föhn (1987), to include additional skier load. I will also introduce the use of weak layers in the snowpack, by calculating surface hoar growth, and implementing this in the skier stability index. Furthermore, I will compare days with observed avalanches to days without observed avalanches to see if there is a significant difference between the two. All estimates/calculations will be done in the forecasting regions used by the present public avalanche forecast in Norway.

1.3 Outline

First, I will introduce background and theory in Chapter 2 to give an understanding of favorable conditions for dry slab avalanches. I will then move on to introducing datasets used, and a deeper understanding of the estimations/calculations done by skier stability index in Chapter 3. Chapter 4 gives results, before moving on to discussing the results found in Chapter 5. Finally, I will conclude my work in Chapter 6, and look at improvements that can be made to the work.

2 | Background

This chapter provides an introduction to snow, snow avalanches and present day forecasting in Norway. Starting of with the formation and structure of snow, in Section 2.1, to get a better understanding of the processes in snow that allows the setup for an avalanche. Further, I will introduce some basics about snow avalanches in Section 2.2, before moving on to the main group of avalanches important for this thesis, dry slab avalanches, in Section 2.3. There, I will introduce the four necessary conditions for a dry slab avalanche to fracture. At last, I will introduce how avalanche forecasting is done in Norway at present day in Section 2.4.

2.1 Snow physics

2.1.1 Snow formation

Snow forms in clouds where the atmospheric temperature is less than 0°C and there is presence of supercooled water (water temperature down to -50°C). Snow begins as an ice crystal which nucleate homogeneously or heterogeneously onto the surfaces of ice nuclei. The basic shape of ice crystals is a hexagonal prism with two basal planes and six prism planes. The relative growth rates of the faces vary with temperature and supersaturation, giving rise to a wide variety of crystal shapes. When the ice crystal grows to a size where it has a significant downward velocity, it becomes a snow crystal. Larger snow crystals continue growing, by accretion or by aggregation, into snowflakes (Armstrong and Brun, 2008). International Commission on Snow and Ice (ICSI) has divided newly fallen snow into nine main groups shown in Table 2.1. Each main group also consists of several subclasses representing rimed and aggregated versions of these forms. The snow is classified by using either a symbol or a two-letter upper case abbreviation code. Subclasses are classified either by using proper symbol or four-letter abbreviation code, where two lower case letters are appended to the main class code (Fierz et al., 2009).

Class	Symbol	Code
Precipitation Particles	+	PP
Machine Made snow	⊙	MM
Decomposing and Fragmented precipitation particles	/	DF
Rounded Grains	•	RG
Faceted Crystals	□	FC
Depth Hoar	∧	DH
Surface Hoar	∨	SH
Melt Forms	○	MF
Ice Formations	■	IF

Table 2.1 – Nine main morphological grain shape classes defined by ICSI (Fierz et al., 2009)

2.1.2 Snow microstructure

Once on the ground, deposited snow particles rapidly bond together to form an ice matrix filled with pores of humid air, and in the case of wet snow, with liquid water (Armstrong and Brun, 2008). Over the winter, the typical snow cover accumulates and develops as a complex layered structure made up of a variety of snow grains, reflecting both the weather and climate conditions. Microstructure of snow is complex, since the size, shape and number of structural elements vary widely in natural snowpack (Fierz et al., 2009). Snow is a porous material, where the pores are interconnected, which gives complex physical properties. This is increased by the fact that the principle component of snow; water, is close to its triple point and can exist in solid, liquid and gaseous phases in the medium. The three phases coexist in a relationship that is strictly governed by laws of thermal and mechanical equilibrium. Snow metamorphism, the change in snow crystal form, can occur rapidly because the crystals are thermodynamically active due to their large surface area to volume ratio and because their temperature is at, or proportionally close to, the melting temperature (Armstrong and Brun, 2008).

Snowfall amounts are measured by depth and snow water equivalent (SWE), which is the depth of snow if it were melted. Combined, the depth and SWE can tell us something about the density of snow. Normal values for snow density is between 100-800 kg m⁻³, ranging from dry, light, new snow, to dense crusts. Blowing and drifting snow and the topography of the underlying ground can lead to considerable spatial variability in the snow depth (Armstrong and Brun, 2008).

2.2 Introduction to snow avalanches

Avalanches can be divided into two main groups; slab avalanches and point release avalanches, illustrated in Figure 2.1.

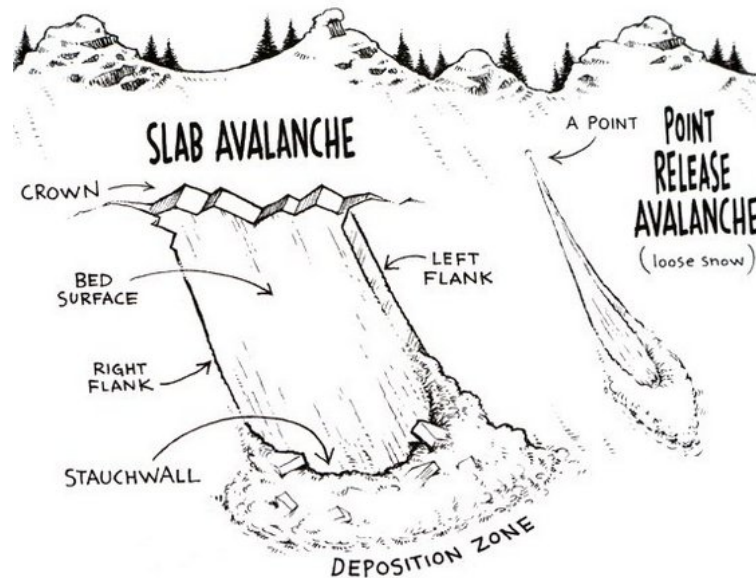


Figure 2.1 – Slab avalanche vs point release avalanche (Clelland and O’bannon (2012))

A point release is when the avalanche starts at a point, releasing snow that moves down the hill, dragging along more snow, creating a fan shape on the hill side. Slab avalanche is a cohesive plate of snow that slides as a unit on the snow underneath (Tremper, 2008). Slab avalanches can have a volume up to 1 million m^3 and reach a speed of 70 m/s (Norem, 2011). The two main groups can be divided into two subgroups - dry and wet. These subgroups are defined by the amount of water in the snow layer. The wet avalanches are more commonly found in spring/summer snow, with higher temperatures and rate of radiation. There is a large difference in the release mechanism of the wet and dry snow avalanches. Dry avalanche releases from stress overloading the strength of the weak layer, whereas in wet avalanches there is a decrease in the strength of the weak layer (Tremper, 2008).

2.3 Dry slab avalanches

As we now have seen, there are big differences in both main groups and subgroups of avalanches, this thesis will focus on dry slab avalanches. There are four necessary conditions for a dry avalanche release; terrain, favorable setup in the snowpack, critical

balance between stress and strength, and a trigger (Tremper, 2008). This section will look closer on each of the following conditions to give a better understanding of what causes an avalanche release.

2.3.1 Terrain

Terrain needs a slope incline that allows for avalanche to start and accelerate. There is no exact lower limit for inclines where slopes are safe, this highly depends on the snow conditions. There are few detailed studies on starting zone inclines, but based on experience McClung (2006) has formed the guidelines shown in Table 2.2. For slab avalanches the favorable slope incline ranges from 25-55°, with highest frequency of avalanches found between 35-45°. Schweizer and Jamieson (2001) found that the mean slope angle for human triggered slab avalanches is between 38° and 39°.

Slope incline	Frequency of avalanche
60-90°	Avalanches are rare; snow sluffs frequently in small amounts.
30-60°	Dry loose snow avalanches.
45-55°	Frequent small slab avalanches
35-45°	Slab avalanches of all sizes
25-35°	Infrequent (often large) slab avalanches; wet loose-snow avalanches
10-25°	Infrequent wet snow avalanches and slush flows.

Table 2.2 – Slope incline guidelines by McClung (2006)

Besides the slope incline, the orientation of the slope to the wind and sun also plays an important role. The amount of sun and radiation affects the snow metamorphism. High amount of radiation increases the speed of melting. Wind, on the other hand, can move large amounts of snow, creating wind slabs (compressed, well-bonded snow) in leeward slopes. Other terrain features that affect the avalanche conditions are; forest cover, ground surface, slope dimension and altitude. In dense forests the snow will not be able to bond to make a cohesive slab. Ground surface affects the binding to the snowpack above, making the snowpack bond poorly to slick surfaces like glaciers or smooth rock surface. For slab avalanche a rule of thumb is that the slope needs to be at least 5 m in height before there is any danger of a slab to release.

2.3.2 Snowpack

Three layers in the snowpack is needed for a dry slab avalanche, which can be seen in Figure 2.2. On top there is the slab, which is a cohesive plate of snow with stronger

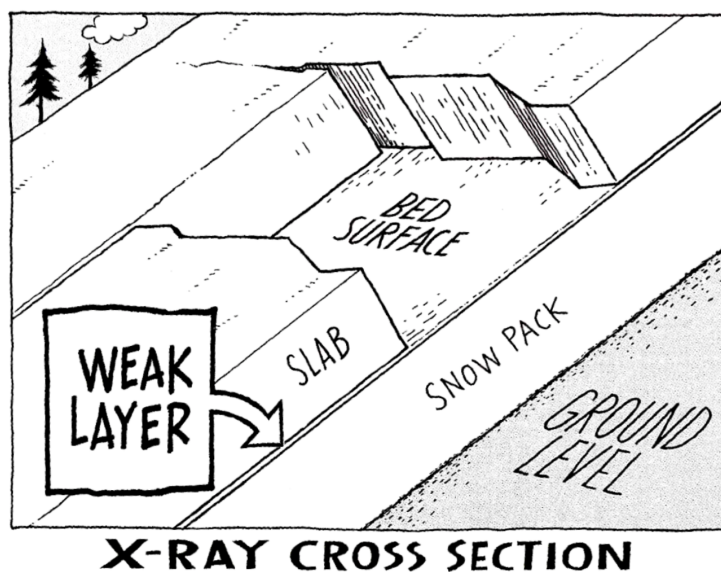


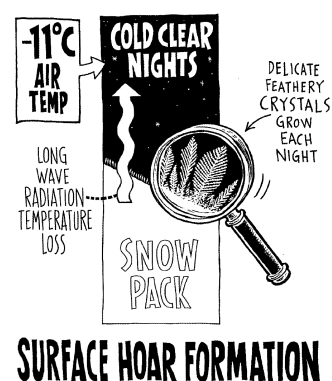
Figure 2.2 – Three-layers of snowpack needed for slab avalanche, illustrated by Clelland and O’bannon (2012)

bindings than the layer below. Cohesion is how well snow grains and crystals are bonded to their neighbors, and the number of bonds per unit volume, which is related to snow density (McClung, 2006). Next, a weak layer or interface, that is less cohesive. A fracture in this weak interface will cause the slab to start sliding. At last, below the weak interface, there is a bed surface for the slab to glide on. This can either be directly on the ground or a harder layer of snow. However, the bed surface does not have to be there prior to the event, an avalanche can create the bed surface after fracture (Tremper, 2008).

Most often avalanches descend on a harder, slicker surface. Some common bed surfaces are; rain crust, sun crust, hard, old snow surfaces, wind hardened snow, and melt-freeze crust (Tremper, 2008)

There is a two-category classification scheme for weak layer forms in relation to avalanche prediction; persistent layer (P) and nonpersistent layer (NP). The classification depends on the crystal form of the snow layer, and how long the layers will remain in the snowpack. Table A.1, in Appendix A, gives a brief description of weak layers and interfaces found in the snowpack.

A weak layer to be particularly aware of is buried surface hoar, described last in Table A.1. This accounts for more human triggered avalanches than any other kind of weak layer (Tremper, 2008). In arctic and subarctic



SURFACE HOAR FORMATION

Figure 2.3 – Surface hoar creation, illustration from Clelland and O’bannon (2012)

latitudes surface hoar grows all day long since the sun is weak in midwinter. The buried surface hoar layer can fail either by collapse or in shear. It can fail in collapse if the new snow is added slowly and the surface hoar crystals remain standing up like columns. If surface hoar layer is critically loaded, just a small trigger can be enough to make the columns collapse. It can also fail in shear when the first snowfall lays the surface hoar crystals over on their side; they remain as a paper-thin discontinuity in the snowpack with very poor bonding across the layer.

2.3.3 Critical balance

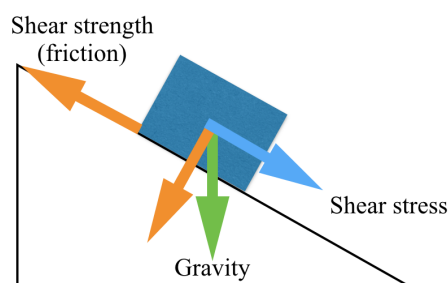


Figure 2.4 – Shear forces acting on a slope.

So far we have the terrain necessary for avalanche conditions. The snowpack is set up for a slab avalanche with a weak layer and a more cohesive slab above it. The next thing we need is a critical balance. Even with a weak layer in the snowpack, the snow can keep stable for a long time. There needs to be a critical balance between the stress and the strength in the snowpack for an avalanche to occur. There are three important questions to ask: what is the stress on the snowpack, where is the strength, and how do we measure this?

Lets cover the easy part first; what is stress?

Shear stress is the force F_{\parallel} acting tangent to the surface divided by the area A on which it acts, see Figure 2.5 (Young et al., 2004) It creates a force per unit area, often denoted with τ . In our snowpack the shear stress is the load of the slab on the weak layer. In other words, it is the stress vector induced by the slab that acts parallel to the cross section of the snow.

Shear strength is the compressive strength (ability to withstand pushing forces) of a soil. It results from two internal mechanisms: cohesion and friction. Cohesion is, as mentioned earlier, the bond strength between snow grains and crystals and number of bonds. Friction refers to the resistance to motion of the snow grains in one layer relative to the grain in another. Friction depends on texture, water content and weight of the snow layers above (which forces the grains together to resist motion) (McClung, 2006). Shear strength of the snow is the strength of the weak layer and how much load it can take before breaking in shear. Because the layering in the snowpack can vary so much, the shear strength is very complex.

Shear stress, as shear strength, is denoted with τ . The difference between shear strength and stress in denotations are marked by tensors, giving the direction of the

force. Shear stress will from now on be written as τ_{xz} , while shear strength will be written τ_s .

We can measure shear strength by doing a shear frame test. This is done by using a shear frame and a pull gauge. A shear frame is a rectangular metal frame with thin cutting edges and crossbars. The shear frame is pressed gently into the snow with the edge parallel to, and a few millimeters above, the weak layer. The gauge is attached to the frame, and a pull is applied rapidly until shear failure occurs. The shear frame index is the force at failure (read on maximum pointer of the gauge) divided by the cross-sectional area of the frame McClung (2006)

The shear frame test gives an indication to what the shear strength is. There are several other field test to give an indication of the balance of stress and strength in the snowpack. Three of the most used tests are; Rutschblock test, column test (CT) and extended column test (ECT). The advantage of these methods is that there is no extra equipment needed from what you would already bring back-country (skis and shovel). The disadvantage is that the test results are not as precise.

Rutschblock test, seen to the left in Figure 2.6 , involves loading a block of snow by a person on skis in several stages. A rectangular block of snow is exposed by shoveling a vertical trench in front and two narrow trenches at the sides. The block is 1.5 m wide in the downslope direction and 2 m wide across the slope. The back is cut with a rope or cord. The trenches and back must be cut at least deep enough to reach the point at which weak layers and weak bonds are suspected. After the block is cut, it is loaded to produce weak layer failure in stages that give a rough numerical rating as an index of stability. After breaking, the column is examined to determine the location and condition of the failure plane, including the type of snow and size of snow grains.

Compression test/CT, seen to the right in Figure 2.6, also needs a column with trenches on the sides, and cut in the back. The column of snow for CT is 30x30 cm and usually no deeper than 100-120 cm, which is the depth a skier would affect the snowpack. A shovel blade is placed on top of the column, and is then added loading in three steps; ten taps from the wrist, ten taps from the elbow and lastly ten taps using the whole arm. The results are recorded along with the total number of taps until failure, and the depth of the layer that failed. Interpretation of the result also include

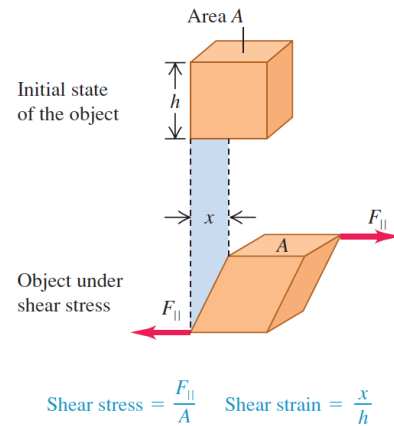


Figure 2.5 – An object under shear stress. Forces are applied tangent to opposite surfaces of the object. The deformation x is exaggerated for clarity. From Young et al. (2004)

a record of shear quality given by McClung (2006);

- Q1 : sudden - clean planar, smooth and fast shear surface.
- Q2: resistant - mostly smooth but block does not slide as readily as Q1
- Q3: break - shear fracture is non planar, uneven, irregular or rough.

The ECT is very similar to the column test, with only notable difference is the size of the column. In ECT the block is 30 cm in direction of the slope, and about 100-120 m wide. The shovel is then placed on top of the column towards one of the sides, and the 30 taps as earlier is completed. The advantage of ECT is that it gives information about the propagation of the fracture in the weak layer.



Figure 2.6 – Rutschblock test(left) and compression test (right), photo from: Schweizer and Jamieson (2004)

2.3.4 Triggers

A trigger can either be natural or human. A human trigger is the load a person puts on the snowpack, either if it is on a snowmobile, skiing, hiking, or in other way putting extra load on the snowpack. Natural triggers can be wind (moving snow, putting extra load on lee areas), snow (high amount of snow on an area will affect the balance between stress and strength), sun (radiation activating metamorphosis processes in the snow pack) rain (rain on a crust layer can make a perfect weak interface, the rain also changes the snow properties, wet snow is heavier, again changing the stress-strength relation), temperature (a big temperature change over a short period of time has great impact on the snow pack), cornice fall and ice fall. (Tremper, 2008).

2.4 Avalanche forecasting in Norway

The Norwegian avalanche forecast is run by NVE and is a collaboration with Norwegian Public Road Administration (NPRA), Meteorological Institute of Norway (MET-Norway), NGI, and Geological Survey of Norway (NGU). On the 14th of January 2013 the first official avalanche forecast was published on www.varsom.no. The first year the avalanche forecast ran, the season lasted from 14th of January to 31st of May. From the following year and forward the season has started 1st December and lasted to 31st of May, with earlier start or later ending if needed (Müller et al., 2013). In the first season forecast were posted four days a week, since then the frequency has increased and at present date forecasts are given daily. (Müller et al., 2013)



Figure 2.7 – Varsom.no



Figure 2.8 – RegObs

In all regions where daily avalanche forecasts are made there is one, or more, local avalanche observer who reports important information about the snow cover. This is done by digging snowpits and examining if there are any weak layers in the snowpack. They also examine the snowpack by conducting stability tests, as described in Section 2.3.3. Local observations are also done and registered by the public through an app made by NVE called regObs. This gives the public the chance to register if they see any warning signs (loud thumping sound in the snow, shooting cracks etc.) or any avalanche activity. They can also register a snow profile, describing if there are any weak layers present in the snow pack.

The forecast is made by a group of three avalanche forecasters and a snow avalanche meteorologist. It is made in two parts; first, the forecasters get a picture of the present situation. This is done from observations made by official observers or reports from the public through regObs. Data from weather stations and weather and snow models are also used. Then the forecast is produced, alongside a special weather forecast for mountain weather. The final forecast, as seen in Figure 2.9, consists of a main message, a written assessment of the snow covers development, 1-3 avalanche problems and danger level on a scale from 1-5 (see Figure 2.10) (Hisdal, 2017).

There are five different types of avalanche problems which are forecasted; persistent layers, wet snow, new snow, glide avalanches, and wind slabs. New snow slabs and loose new snow are subgroups of new snow. Persistent layers and deep persistent layers are subgroups of persistent layers, and wet slab avalanches and loose wet avalanches are

subgroups of wet snow.

varsom.no

Avalanche forecast for Voss Friday 2018-05-04

Norwegian avalanche, flood and landslide hazard warnings > Avalanche bulletins > Avalanche forecast for Voss Friday 2018-05-04

24.04 25.04 26.04 27.04 28.04 29.04 30.04 01.05 02.05 03.05 04.05 05.05 06.05

Published: 2018-05-03 03:22 PM

2 Moderate Be careful in steep slopes and in high north facing areas with dry wind slabs. Avoid areas below glide cracks.

Avalanche problems and travel advice

Loose wet avalanches
Loose snow
Be careful in avalanche release and runout areas. Avoid skiing in terrain traps. Timing is important. Stability decreases when the snow surface gets wet and soft. Wet snow avalanches tend to release spontaneously.

Wet slab avalanches
Water pooling in/above snow layers
Avoid staying for a longer period in avalanche release and run out areas. Wet snow avalanches tend to release spontaneously. Stability decreases when the snow surface gets wet and soft. Timing is important.

Storm slab avalanches
Buried weak layer of new snow
Be careful in steep slopes and around terrain traps until the new snow has stabilized. The avalanche problem is generally widely distributed on any steep slope with deep new snow. Look for cohesive new snow that breaks apart or is poorly bonded to the old snow. Cracks around your skis are a typical dangersign.

For safer travel:
The bulletin does not include a detailed text about the avalanche conditions. [This is only given in Norwegian](#). Translate it using [google translate if you like](#). The text result will be informative, and most likely amusing.
For planning your trip and recognizing avalanche terrain, use [maps](#).
Norway has 1:50 000 maps for the whole country. Maps can be bought at bookstores and sports shops, or printed from the net.
Visit [www.ut.no](#) for topographic maps online. For slope angle maps, see [NGU slope angle maps](#) ("heining" means slope angle).
Modelled snowpack and historic and current weather information can be found on the webpage [varsom.no](#). This site uses information from the weather stations and interpolate values from the stations for gridded maps.
Detailed weather forecast can be found online at [www.vr.no](#) or [www.storm.no](#). Vr.no is also in English, but the weather in text format is only given in Norwegian.

European Avalanche Warning Services
www.avalanche.no

Figure 2.9 – Example of avalanche forecast for the region of Voss from varsom.no. Showing the forecast danger level for 10 days prior to date, date and day after. There is a short text about the general forecast, before it tells what avalanche problems that are valid in the region, in what aspects and what elevations you might encounter them. Not included in the picture is the mountain weather forecast posted just below. As can be seen mentioned in the text box on the right hand side, the English version is less detailed than the forecast given in Norwegian.






North American Public Avalanche Danger Scale Avalanche danger is determined by the likelihood, size and distribution of avalanches.				
Danger Level		Travel Advice	Likelihood of Avalanches	Avalanche Size and Distribution
5 Extreme		Avoid all avalanche terrain.	Natural and human-triggered avalanches certain.	Large to very large avalanches in many areas.
4 High		Very dangerous avalanche conditions. Travel in avalanche terrain <u>not</u> recommended.	Natural avalanches likely; human-triggered avalanches very likely.	Large avalanches in many areas; or very large avalanches in specific areas.
3 Considerable		Dangerous avalanche conditions. Careful snowpack evaluation, cautious route-finding and conservative decision-making essential.	Natural avalanches possible; human-triggered avalanches likely.	Small avalanches in many areas; or large avalanches in specific areas; or very large avalanches in isolated areas.
2 Moderate		Heightened avalanche conditions on specific terrain features. Evaluate snow and terrain carefully; identify features of concern.	Natural avalanches unlikely; human-triggered avalanches possible.	Small avalanches in specific areas; or large avalanches in isolated areas.
1 Low		Generally safe avalanche conditions. Watch for unstable snow on isolated terrain features.	Natural and human-triggered avalanches unlikely.	Small avalanches in isolated areas or extreme terrain.
Safe backcountry travel requires training and experience. You control your own risk by choosing where, when and how you travel.				

Figure 2.10 – Avalanche danger scale used internationally

3 | Data and method

Through this chapter the data sets and methods used in this thesis will be presented. First, describing the data sets containing meteorological and snow cover data. Followed by a description of the area of interest, and data sets used to divide the country into forecast regions. Finally, the methods used to calculate Skier stability index (S') are presented .

3.1 Data

3.1.1 Snow cover data

Snow cover, air temperature and precipitation data has been provided by NVE. Variables used from the data set are shown in Table 3.1. The NVE data has a 1 km spatial resolution and 24 h temporal resolution. Air temperature and precipitation are based on observations, while snow-cover data is modeled using the seNorge snow model(Lussana et al., 2018a,b). The model uses a threshold temperature to separate between snow and rain precipitation, it handles separately the ice and liquid water fractions of the total SWE, and keep track of the total accumulation and melting of snow.

Short name	Long name	Unit
tm	Air Temperature	°C
rr	Precipitation	mm
sd	Snow Depth	mm
swe	Snow Water Equivalent	mm
fsw	Fresh Snow Water Equivalent	mm
sdfsw	Snow Depth Fresh Snow	mm

Table 3.1 – Variables used from NVE

Air temperature is collected from approximately 230 weather stations in Norway.

From these the 24 h-middle temperature is calculated and interpolated over a grid with 1 km point distance. The interpolation is based on the Bayesian method where the background field describes the large scale situation in the atmosphere (Engeset, 2016; Lussana et al., 2018b).

Precipitation is collected from approximately 400 stations, where the accumulated precipitation is calculated. Precipitation is, as air temperature, interpolated over a 1 km grid using the Bayesian method. It also uses the Optimal Interpolation (OI) method interpolating on a scale from coarse to fine (Engeset, 2016; Lussana et al., 2018a).

Snow water equivalent SWE is calculated with a snow model using the daily average of temperature and precipitation (Engeset, 2016; Lussana et al., 2018a).

Snow depth is calculated from the simulated SWE and the density of the snow. The fresh snow density and compression caused by weather conditions are taken into account in the simulation (Engeset, 2016; Lussana et al., 2018a).

3.1.2 Meteorological data

Additional meteorological data used is provided by MetCoOp Ensemble Prediction System (MEPS). MEPS is a cooperation between Meteorological Institute of Norway (MET Norway), Sweden Meteorological and Hydrological Institute (SMHI) and the Finnish Meteorological Institute (FMI) (Mueller et al., 2017). The core of the model is based on the AROME (Applications of Research to Operations at Mesoscale) model developed by Meteo-France (Mueller et al., 2017). MEPS has a horizontal resolution of 2.5 km and 65 vertical layers. The model has four main cycles (00, 06, 12 and 18) at which point a 66 h forecast is produced. For this thesis I have used the analysis of each main cycle. Variables used from MEPS can be seen in Table 3.2.

Short Name	Long Name	Height(m)	Unit
T0M	Surface temperature	0	K
T2M	Screen level temperature	2	K
RH2M	Screen level relative humidity	2	%
U10M	Zonal 10 meter wind	10	
V10M	Meridional 10 meter wind	10	ms ⁻¹

Table 3.2 – Variables used from MEPS

3.1.3 Avalanche history record

The avalanche history record is a collaboration between observations done by government agencies and private persons. Agencies contributing to the record are Geological Survey of Norway (NGU), Norwegian Geotechnical Institute (NGI), Norwegian National Rail Administration (JBV), and Norwegian Public Road Administration (NPRA). Public registrations have been done through regObs, mentioned in Section 2.4, and skredregistrering.no. The earliest observations recorded are done by NGU, a rock slide which dates back to before year 1000. JBV has been registering avalanches along railroads since 1920, while NPRA has been registering avalanches along roads since 1973 (Norges Vann- og Energiressurser, 2017). The avalanche record contains all types of avalanches, from rock slides to cornice fall. For this thesis, we only look at avalanches with the attributes of snow avalanche (excluding cornice fall). The 10 snow avalanche attributes registered can be seen in Table 3.3. Only avalanche data from the forecasting season (1th December - 31th May) between the winter 2014 and winter 2017 will be included in the evaluation. Figure 3.1 gives the distribution of the 10 snow avalanche attributes for this period. The time error for observation is lower for recent data than earlier. Highest uncertainty for avalanche observations in the chosen period is found to be ± 1 day.

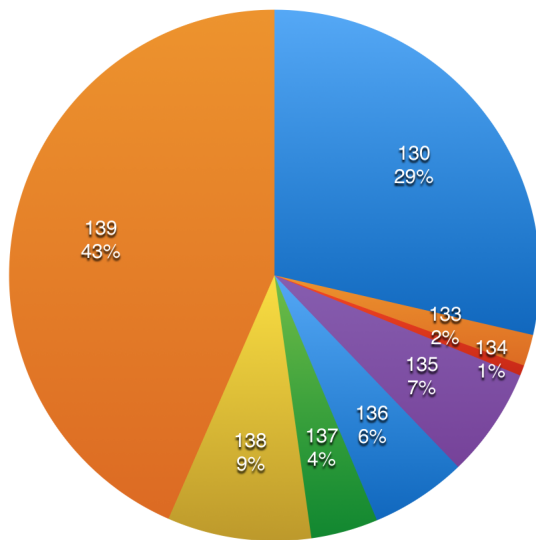


Figure 3.1 – Distribution of 2202 snow avalanches recorded during the forecasting periods (1st Dec - 31st May)

Code	Description
130	Snow avalanche, unspecified
131	Snow avalanche, wet
132	Snow avalanche, dry
133	Slush avalanche
134	Point release, unspecified
135	Point release, wet
136	Point release, dry
137	Slab avalanche, unspecified
138	Slab avalanche, wet
139	Slab avalanche, dry

Table 3.3 – Snow avalanche observation classification in NVE avalanche history record

The avalanche records are purely from observations, meaning that there will be a

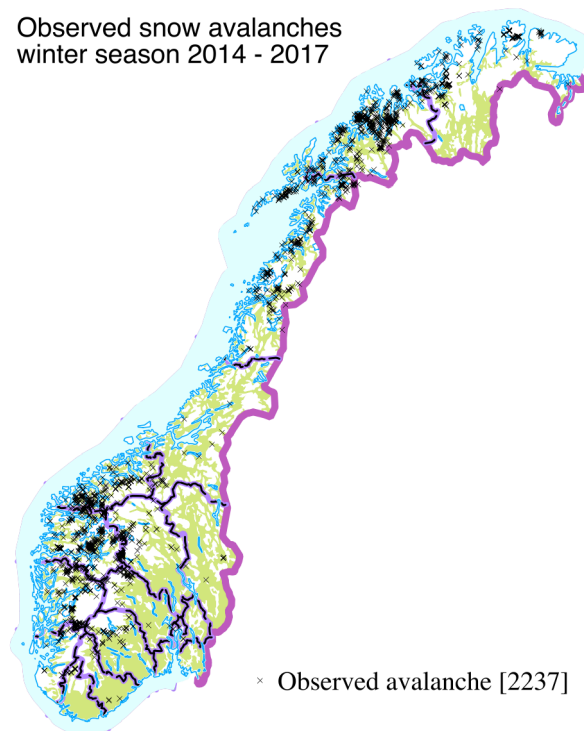


Figure 3.2 – Observed avalanches in winter seasons (1st December - 31st May) 2014-2017

lack of data for remote areas. Future use of satellite and radar observations can give a better understanding of avalanche activity in remote locations.

3.2 Area of interest/focus

3.2.1 Forecast regions

In the national avalanche forecast, Norway is divided into 46 regions, which again is given priority A and B, shown in Table 3.4. The 21 A-regions have daily avalanche forecasts during the whole forecast period, while the B-regions receive forecast on days with danger level 4 or 5. Figure 3.3 is an example on how the daily forecast is portrayed on varsom.no, where the 21-A regions can be seen with the forecasted avalanche danger, while the B-regions can be seen outlined in black (Varsom.no, 2017; Hisdal, 2017).

3.2.2 Avalanche deployment areas

To avoid including areas with terrain below 30° , NVEs deployment area map for snow avalanche has been used. Deployment area consists of regions with terrain steeper than 30° . The map is made from a nationwide terrain model with a resolution of 25 m, with primarily 20 m height contours. This causes some limitations, as steep slopes lower

Avalanche forecast regions	
A regions	B regions
Hallingdal	Akershus
Hardanger	Aust-Agder
Indre Fjordane	Buskerud sør
Indre Sogn	Finnmarskysten
Indre Troms	Finnmarksvidda
Jotunheimen	Hedmark
Lofoten and Vesterålen	Helgeland
Lyngen	Hordalandskysten
Nord-Troms	Nord-Trøndelag
Nordenskiold Land	Nord-Gudbrandsdalen
Ofoten	Oppland sør
Romsdal	Oslo
Salten	Sør-Finnmark
Sør-Troms	Østfold
Sunnmøre	Rogaland
Svartisen	Sør-Trøndelag
Trollheimen	Svalbard øst
Troms	Svalbard sør
Vest-Finnmark	Svalbard vest
Vest-Telemark	Telemark sør
Voss	Vest-Agder
	Vestfold
	Ytre Fjordane
	Ytre Nordmøre
	Ytre Sogn

Table 3.4 – Avalanche forecasting regions. A regions - daily forecast between 1st December and 31st May. B regions - forecast when danger level is 4 or 5.

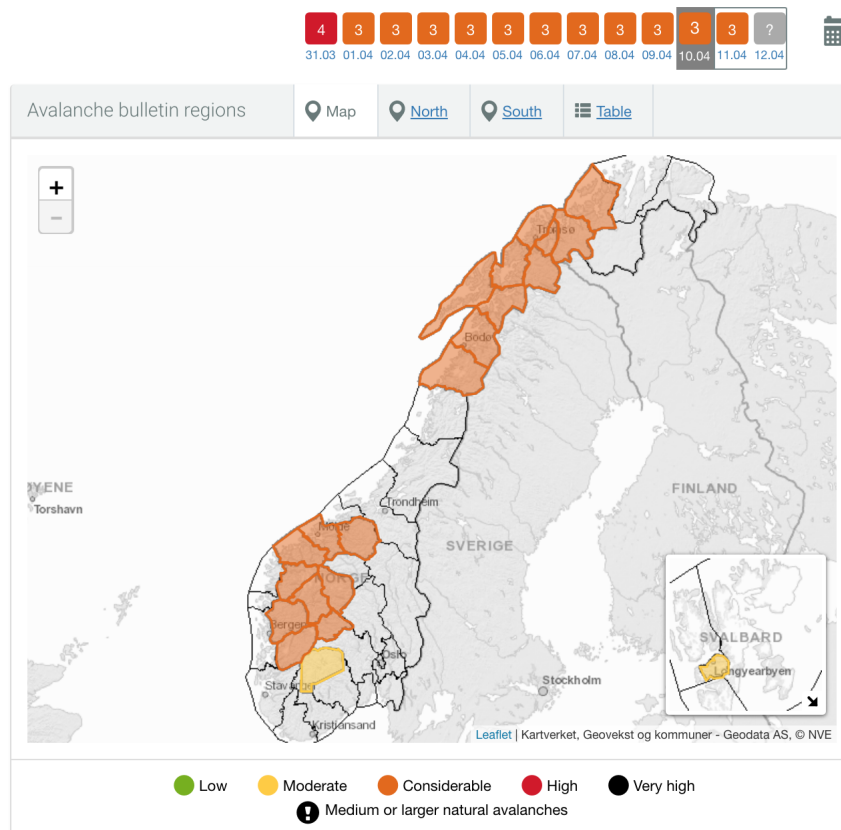


Figure 3.3 – Avalanche forecast for 10.04.18. 21 A-regions showing forecast avalanche danger for the day, while the B-regions can be seen outlined. The avalanche forecast is gathered from Varsom.no (2018a)

than 20 m is not implemented in the map, as well as some slopes between 20 and 50 m (Peereboom, 2015). Figure 3.4 shows the deployment areas for the region of Voss shaded in dark red. In the figure the run-out zones of snow avalanches are also shown in lighter pink.

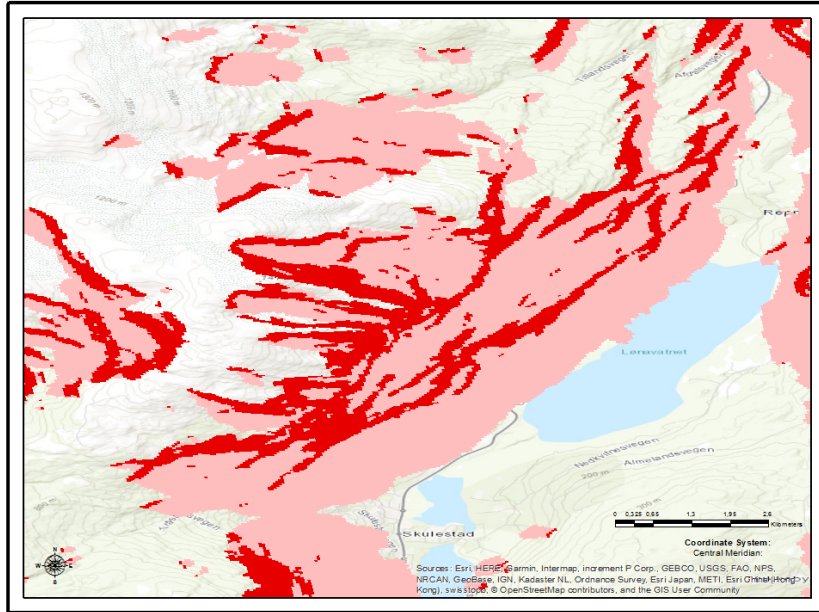


Figure 3.4 – Example of deployment regions used. Deployment areas are shaded dark red, while run-out zones, the length an avalanche can travel, are shaded in lighter red. The area shown is located in the region of Voss

3.3 Method

3.3.1 Stability index S

As seen in Chapter 2 one of the necessary conditions for a slab avalanche is a critical balance between strength and stress in the snowpack. One of the earliest attempts of modeling the ratio was done by Roch (1966a), who defined a Stability Index (S) as

$$S = \frac{\tau_s}{\tau_{xz}} \quad (3.1)$$

where τ_s is the shear strength of the weakest layer and τ_{xz} is the shear stress component parallel to the slope at a given slope location. Assuming the normal load effect, load perpendicular on the surface, was due to internal friction, ϕ , Roch (1966a,b) expressed the adjusted shear strength as

$$\tau_s = \Sigma + \sigma_{zz}\phi \quad (3.2)$$

where Σ is the maximum pull force divided by the area of the shear frame, and the normal stress(perpendicular to the surface) on the weak layer expressed as

$$\sigma_{zz} = \rho gh \cos^2 \Psi. \quad (3.3)$$

due to slab density (ρ), slab thickness (h) measured vertically on a slope of inclination Ψ (as seen in Figure 3.5).

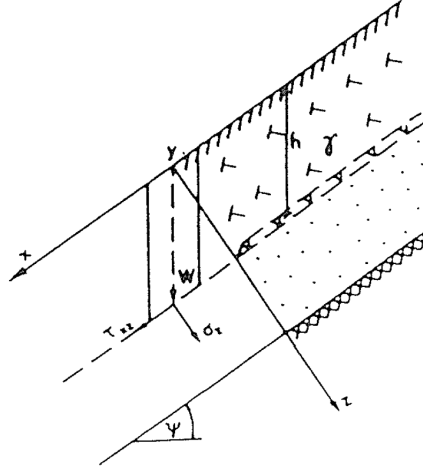


Figure 3.5 – Slab avalanche coordinate system (Föhn, 1987)

Roch (1966a) found that the internal friction term depend on strength and microstructure. Through share frame tests he determined empirical formulas for ϕ for several different microstructures. During the winter of 1995, Jamieson (1995) tested the shear strength for three persistent layers and one non-persistent layer. He found that for persistent layers the increase in strength for an increase in normal load is not significant, giving no adjustment for normal load ($\phi = 0$). For non-persistent layers, the strength measurements obtained with 0.01 m² and 0.025 m² shear frame are adjusted to the equivalent strength of a very large specimen, called the Daniels strength. The strength measurements obtained with 0.025 m² frame are multiplied by the adjustment factor, 0.65, to obtain the Daniels strength. This gives the equations of ϕ for precipitation particles

$$\phi(\Sigma_{\infty}, \sigma_{zz}) = 0.08\Sigma_{\infty} + 0.056 + 0.022\sigma_{zz} \quad (3.4)$$

and for decomposed and fragmented precipitation particles as well as for rounded grains

$$\phi(\Sigma_{\infty}, \sigma_{zz}) = 0.08\Sigma_{\infty} + 0.224 \quad (3.5)$$

The shear strength of dry snow is strongly related to density and grain form (Jamieson and Johnston, 2001). Perla et al. (1982) gave the relation for density to shear strength

$$\Sigma_{\infty} = A \left(\frac{\rho}{\rho_{ice}} \right)^B \quad (3.6)$$

where ρ_{ice} is the density of ice (917 kg m⁻³) and A and B are empirical constants that depend on grain form. These can be seen in Table 3.5.

Grain form	A	B
Precipitation particles	14.5	1.73
Decomposed/fragmented	14.5	1.73
Rounded grains	14.5	1.73
Faceted crystals	8.5	1.48
Depth hoar	8.5	1.48

Table 3.5 – Strength-density regression by grain form by Jamieson and Johnston (2001)

Given the adjusted normal loads and shear strengths, Equation 3.1 becomes

$$S = \frac{\tau_s}{\tau_{xz}} = \frac{\sum_{\infty} + \sigma_{zz} \phi(\sum_{\infty}, \sigma_{zz})}{\rho g h \sin \Psi \cos \Psi} \quad (3.7)$$

3.3.2 Skier stability index S'

Föhn (1987) added an artificially induced stress, $\Delta\tau_{xz}$, to the stability index defined by Roch (1966a), to obtain an index for artificially triggered avalanches. The added stress represents a human trigger, as mentioned in Section 2.3.4. This can be any load added by a skier, a snowmobile or other load from humans.

$$S' = \frac{\tau_s}{\tau_{xz} + \Delta\tau_{xz}} \quad (3.8)$$

For a skier, the triggering point is calculated as a line load. Assuming a stress-free surface and elastic behavior of the snow, the shear stress is calculated by the stress-functions of Airy (Föhn, 1987).

$$\Delta\tau_{xz} = \frac{2L \cos \alpha_{max} \sin \alpha_{max}^2 \sin(\alpha_{max} + \Psi)}{\pi h \cos \Psi} \quad (3.9)$$

where L is the line load due to a skier ($L = \frac{m*g}{l} = \frac{75 \text{ kg} * 9.81 \text{ m s}^{-2}}{1.7 \text{ m}}$) and α_{max} is the angle for peak shear stress induced by the skier on the snow surface. As seen in Figure 3.6, the angle is tilted downward. The peak value of α_{max} is found by differentiating $\Delta\tau_{xz}$ with regards to α to find the magnitude and position of the maximum stress induced from the human trigger. For a slope angle of $\Psi = 38^\circ$, angle of peak stress $\alpha_{max} = 54.34$.

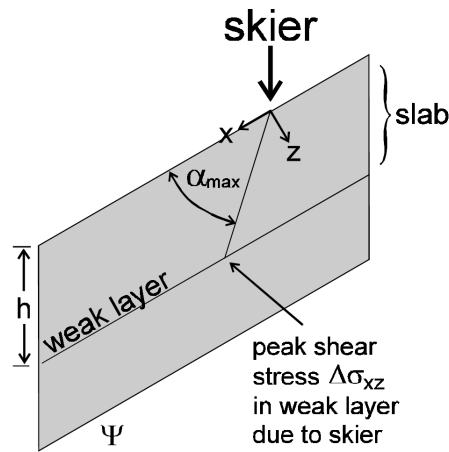


Figure 3.6 – Cross section of slab showing peak stress induced by static skier (Jamieson, 1995)

Skier stability index (S') is calculated in three different methods, which can be seen in Table 3.6.

Version	Description	R	D	P
v1	Homogeneous snow cover. $h = sd$, density = swe/h . NP	x	x	
v2	Two "layered", calculating for different snow density in fresh snow. $h = sd$, $\rho = (sd*swe + sdfsw*fsw)/h$. NP	x	x	x
v3	Surface hoar implemented. Snow depth is accumulated snow cover since last surface hoar layer.	x		

Table 3.6 – Skier stability index (S') versions 1-3 with short name of data used from Table 3.1 and what areas the versions are estimated in; R - full forecasting regions, D - forecasting regions, only grids inside deployment areas, P - around point of observed avalanche

3.3.3 Surface hoar formation from latent heat flux

Surface hoar growth is common on clear winter nights when radiative cooling lowers the surface temperature of the snow (Horton et al., 2014). Crystal growth requires a replenished moisture supply that may be provided by light drainage winds (Horton et al., 2014; McClung, 2006) and a high temperature gradient (inversion) above a snow surface that is chilled below the ice point (McClung, 2006). Surface hoar crystals can shrink from incoming solar radiation, strong winds, warm air advection and rain.

Latent heat flux modeling

The latent heat flux is modeled by using the bulk aerodynamic method (Stull, 1988, p. 262), which assumes, under neutral atmospheric conditions, the latent heat flux Q_E can be approximated by

$$Q_E = 0.62C_e \frac{\rho_a}{P} w (\omega e_S(T_A) - e_S(T_S)) \quad (3.10)$$

where C_e is the bulk transfer coefficient, ρ_a is the density of air, P is air pressure, w is wind speed, ω is relative humidity and e_s is the saturation vapor pressure over ice at air T_A and surface T_S temperatures. C_e depends on wind speed, aerodynamic roughness and atmospheric stability. For this study we will use an average value of 2.9×10^{-3} found by Hachikubo (2000). In addition, standard atmospheric values of air density (1.01 kg m^{-3}) and air pressure (90.4 kPa).. The saturation vapor pressure over ice was calculated with the Clausius-Clapeyron equation

$$e_S(T_{A/S}) = 611 \text{ kPa} \exp \left(6139 \text{ K} \left(\frac{1}{273} - \frac{1}{T_{A/S}} \right) \right) \quad (3.11)$$

Positive values of Q_E corresponds to deposition of vapor (surface hoar growth) and negative values to sublimation.

Surface hoar growth

Surface hoar growth is estimated by integrating the latent heat flux for each day. Assuming no surface hoar growth on days with precipitation and days with negative Q_E . For days with no precipitation, and positive Q_E an average growth rate of 2.1 mm pr day is assumed. The average growth rate used was found by Horton et al. (2014) in an observational study done in Canada over 7 winters (2005-2012). The growth rates were found by applying linear fits to observed crystal size against number of precipitation free days (from weather stations and weather modeled data).

3.3.4 Descriptive statistics

To evaluate the results found from skier stability index, i will use some statistical methods. The different methods used are explained below.

Center

There are different forms of finding the center of a dataset, the two methods used in this thesis is the mean and median. Mean is calculated by

$$\bar{x} = \frac{1}{N} \sum_{i=1}^N x_i \quad (3.12)$$

where N is the number of samples.

The median is the middle value in a set of numbers arranged according to magnitude. Separates the higher half from the lower half of the data set. In a series $x = [1\ 2\ 2\ 4\ 5\ 7\ 8]$ the median value is 4 (Thomson and Emery, 2014).

Dispersion

The dispersion is the extend distribution is stretched or squeezed. Same unit as the quantity being measured.

Standard deviation

$$s = \sqrt{\frac{1}{n-1} \sum_{i=1}^n (x_i - \bar{x})^2} \quad (3.13)$$

where n is the number of samples and \bar{x} is the mean value of data. In normal distribution standard distribution spans approximately 68 % of the measurements, two standard deviations spans 95 % of the measurements (Thomson and Emery, 2014).

4 | Results

In this chapter I will present the results from the method I described in Chapter 3. First I will present sensitivity analysis of the calculations done. After this, the results from surface hoar growth will be presented. Then I will move on to look at the skier stability index, for the three versions introduced in Section 3.3.2.

4.1 Sensitivity Analysis

With input data with spatial resolution between 1 km and 2.5 km, we can expect there to be large variances of the data inside a grid in reality. To get a better understanding of how the main calculations are affected by this variance, I will in this section perform a sensitivity analysis of Skier stability index (S') and Q_E . The sensitivity analysis is conducted by differentiating the equation of interest with respect to the individual input variables, while the other variables are kept fixed. This will give us a better understanding of what input will affect the calculations the most.

4.1.1 Sensitivity analysis of Skier Stability Index

For S' , the variables to investigate are snow density (ρ), layer thickness (h), slope angle (Ψ), mass of skier (m), and ski length (l). The result of the sensitivity analysis is seen in Figure 4.1. An interesting factor to investigate is whether the variable improves stability, S' increases, or weakens it, S' decreases, as it changes. Negative values of the derivative are equivalent to a decrease in stability, while positive values increase the stability.

We can group the five variables into strengthening and weakening variables of snow stability. Snow height (b), slope (c), and skier load (d) are the variables that weaken the stability. An important factor to notice is the scale differences in the rate of change. We can see that the mass of skier is in a factor of 10^{-2} lower than the other values. An error in input data of skier mass will not have a crucial effect on the results of S' . The difference seen between nonpersistent layer (NP) and persistent layer (P) can look greater than they are because of the low scale. Next up, snow height, increase in height

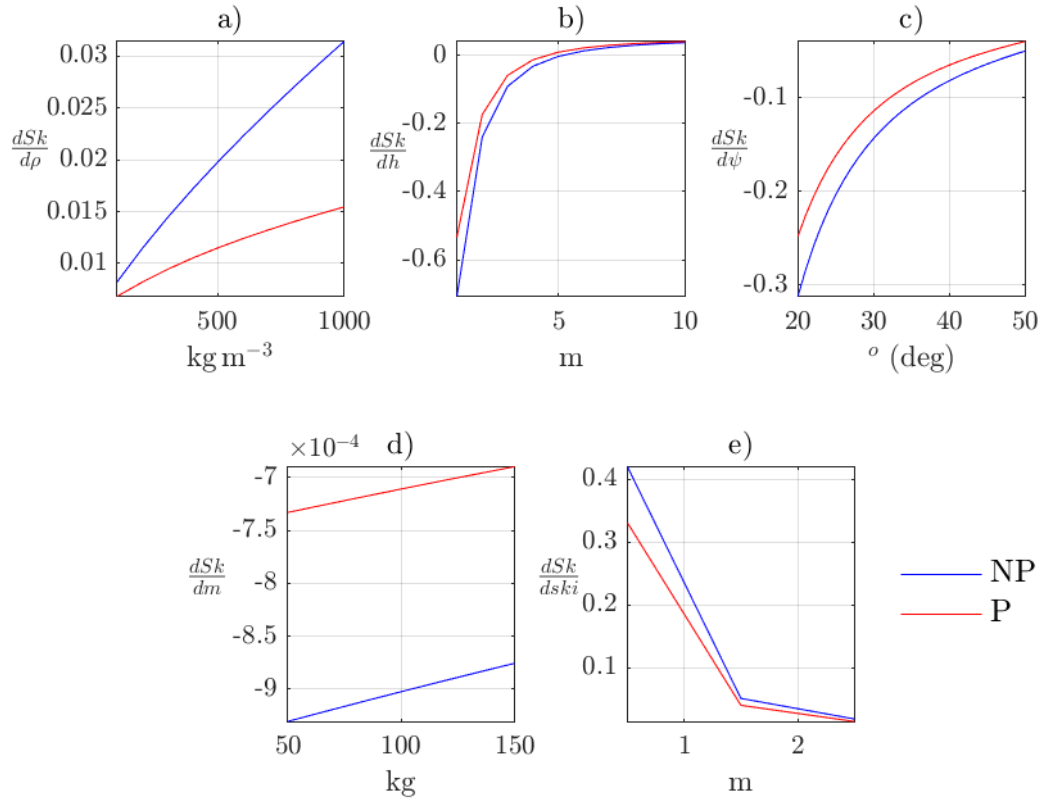


Figure 4.1 – Skier stability index sensitivity to change by different parameters. From top left; a) snow density, b) snow height, c) slope, d) mass of skier, e) length of ski. Fixed values used for the runs are $\Psi = 38$, skiers mass = 75 kg, ski length = 1.5 m, snow height = 2m, rho = 300 g/cm^3 ;

will lead to a decrease in skier stability until it reaches a critical point at 5m depth, where the stability starts to increase again. Snow layers most often between 0-5m. When the snow heights are low, an error in input data will lead to a more significant error in the final S' . This is the same as for slope, lower slopes give higher uncertainties in the outcome.

Stabilizing factors are density and ski length. Density is in a factor of 10 lower than other values. Higher values of density will give large uncertainties in S' with uncertainties in input data. Ski length has a jump at 1.5m, load much more direct with shorter values. As this thesis focus on skier load, an average ski length (for an adult) will be between 1.7m and 2m, in this range S' is not as sensitive.

4.1.2 Sensitivity analysis of Q_E

As for S' , the input data for Q_E has a spatial resolution that leaves room for uncertainty in the measurements. In this case the variables of interest are; surface temperature (T_S),

air temperature (T_A), relative humidity (ω), wind speed (w), bulk transfer coefficient (C_e), air density (ρ_a), and air pressure (P). Results for the sensitivity analysis can be seen in Figure 4.2. RH, wind speed, ρ_a and C_e are all linear variables of Q_E , with values (see Table 4.1).

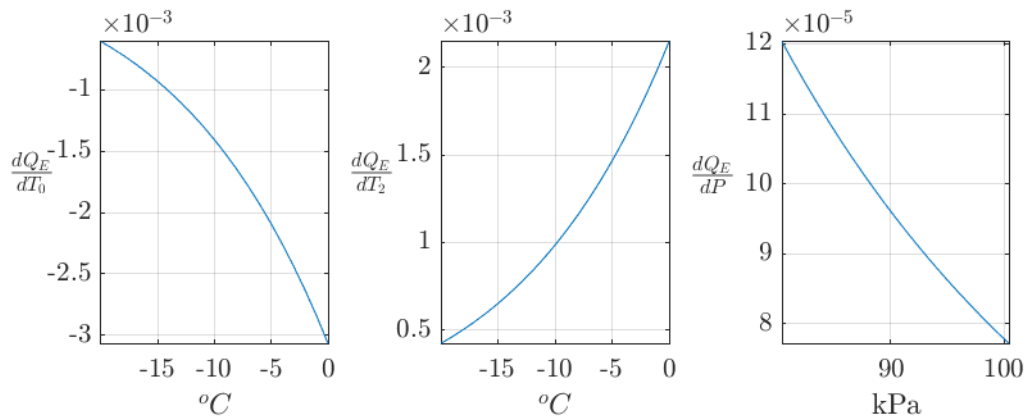


Figure 4.2 – Sensitivity analysis of Q_E . Left panel shows surface air temperature(0m), middle panel: air temperature (2m), and last right panel: air pressure. Fixed values used when calculating; air temperature 270, surface temperature 270, wind speed 3, air density 1.01, air pressure 90.4kPa, rh 70%, and C_e 2.9e-3.

Grouping the variables into increasing and decreasing factors again we can see that Air temperature and air pressure are the increasing effects, stronger heat flux with lower higher temperatures., and lower higher pressure. As for S' , it is important to pay attention to the scale of change. We can see that the temperature changes (both air and surface) plays a much bigger role in the change of Q_E . The variables in Table 4.1 have a constant rate of change. RH increases Q_E , while the three other variables leads to a decrease of Q_E . Most affected by RH, wind speed and air density are in the same factor as air/surface temperature.

Variable	Value
RH	0.0287
Wind speed	-0.0029
Air density	-0.0085
C_e	-2.9670

Table 4.1 – Derivatives with constant values, using same fixed values as in Figure 4.2

4.2 Surface hoar growth

Surface hoar growth has been calculated in each A-region for the winter seasons 2014-2017 using daily averages of Q_E to calculate the daily surface hoar growth. Figure 4.3 shows the mean surface hoar growth formation in region of Voss for the winter season 2014. The Q_E and surface hoar is first calculated in each 1 x 1 km grid by the input data, before averaging over the region. This gives the indication that there is surface hoar growth on days with negative Q_E .

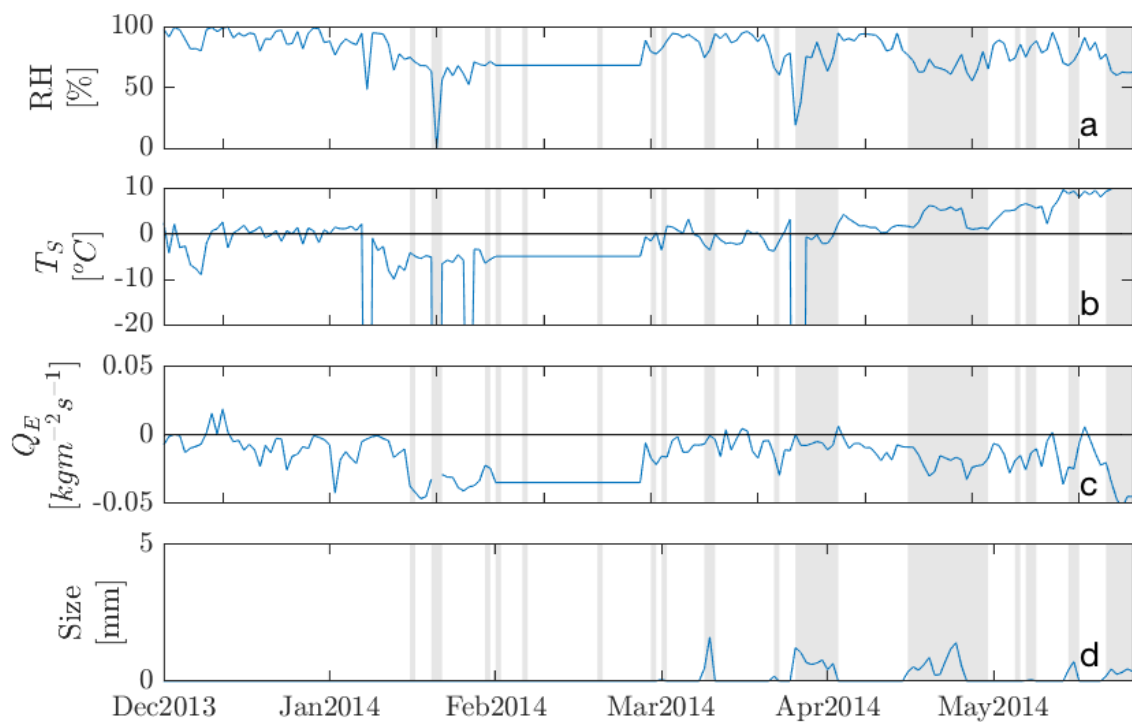


Figure 4.3 – Mean weather data from MEPS over region of Voss for winter season 2014 including a) relative humidity(RH) b) surface temperature (T_S) c) latent heat flux Q_E and d) modeled surface hoar size. Shaded areas represent precipitation-free periods identified by NVE-data.

To see if there are any correlations between precipitation and observed avalanches or between surface hoar growth and observed avalanches these have been plotted together in Figure 4.4.

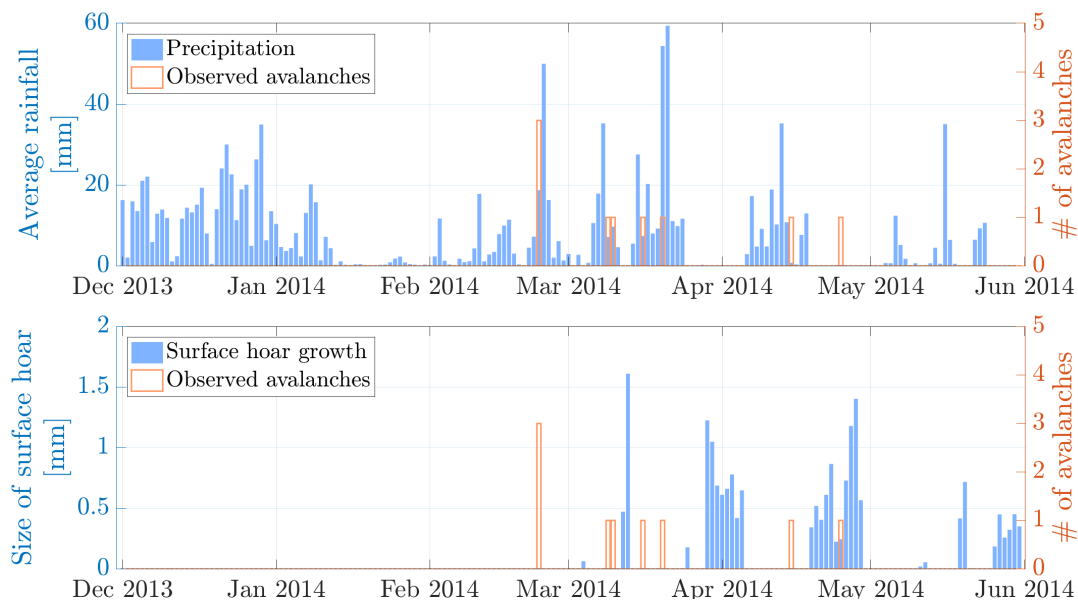


Figure 4.4 – Top panel: daily average precipitation (blue) and number of observed avalanches (orange) for the region of Voss winter season 2014. Bottom panel: surface hoar growth in mm (blue) and observed avalanches (orange). Surface hoar size has been calculated by assuming a constant growth rate on days with positive Q_E

4.3 Skier Stability Index (S')

Skier stability index (S') is calculated for the A regions (Table 3.4) for the four winter seasons 2014-2017. S' is run for the three versions introduced in Table 3.6, and assuming a constant slope of 38° . Briefly repeated; v1, assumes a homogeneous snowpack, v2, adds the effect of density difference to the new fallen snow, still estimating with full snow depth, v3, implements the surface hoar layer. Both v1 and v2 assumes nonpersistent layer (NP). In v3, the snow depth is estimated by accumulating the new snow (sdfsw, Table 3.1) between days of surface hoar growth. For every day with surface hoar growth a new snow layer is created. As mentioned in Section 2.3, buried surface hoar layers are considered a persistent layer (P).

We will now compare the three versions estimated in two regions, Voss and Lyngen. Figure 4.5 and 4.6 gives v1 and v2 for the two different spatial resolutions, as well as v3 region. The figure gives the timeline for four winters (2014-2017) in regions Voss and Lyngen, respectively. V1 and v2 calculated for full regions can be seen in green, while deployment calculated v1 and v2 are given in purple. Lighter colors showing v1, and darker for v2. V3 is shown in blue. Throughout all the time series there is a clear coupling between the two v1 runs, and the two v2 runs. While for Voss (Figure 4.5) the deployment area shows generally more stable S' , in Lyngen (Figure 4.6) the full region is generally more stable. A common trait to the figures is the difference in fluctuation

between v1 and v2. For both regions v2 gives a smoother curve, and v1 shows larger fluctuations. V3 shows an overall unstable situation, with high fluctuations.

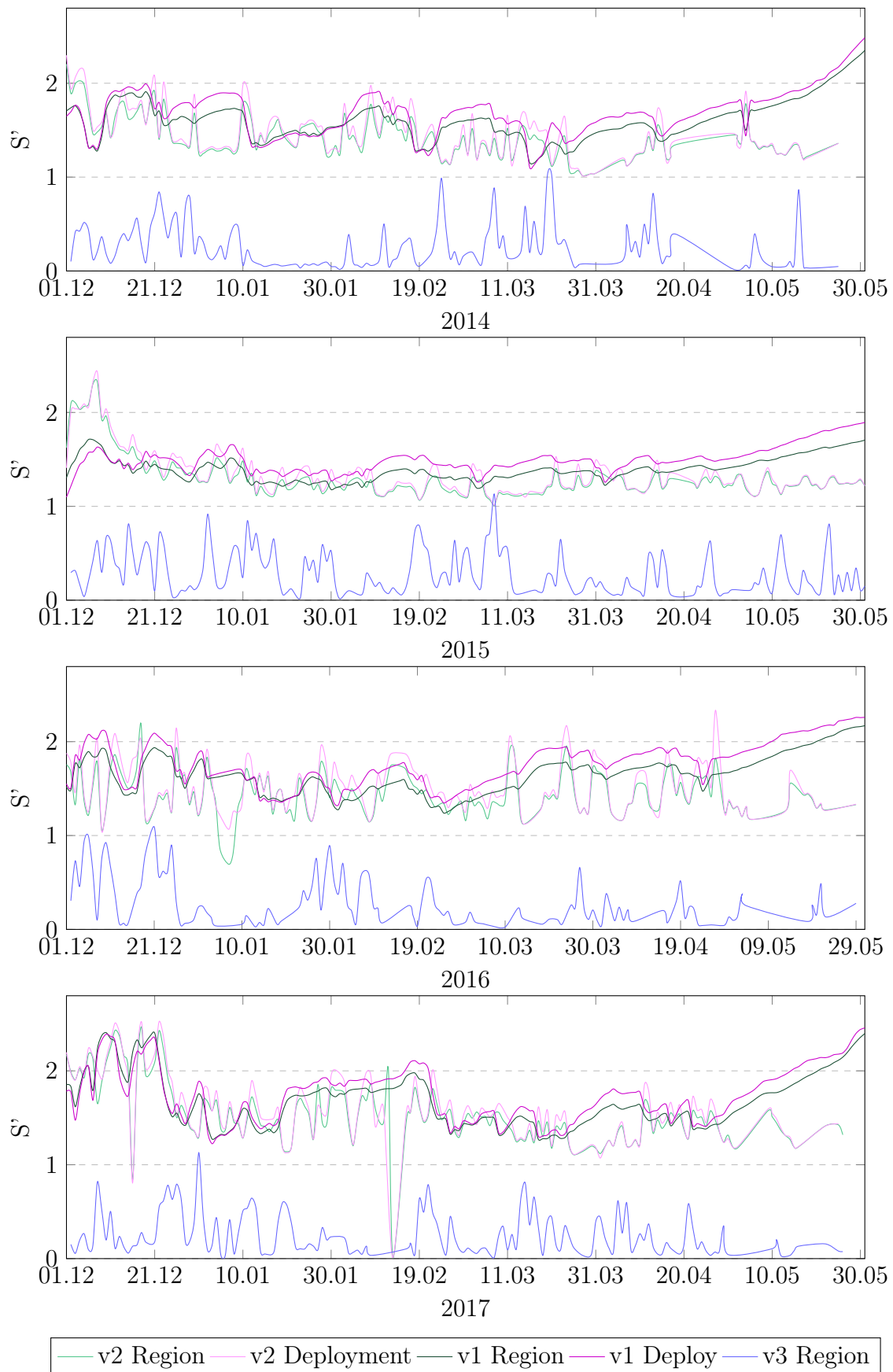


Figure 4.5 – Mean skier stability index for the four winter seasons in Voss.

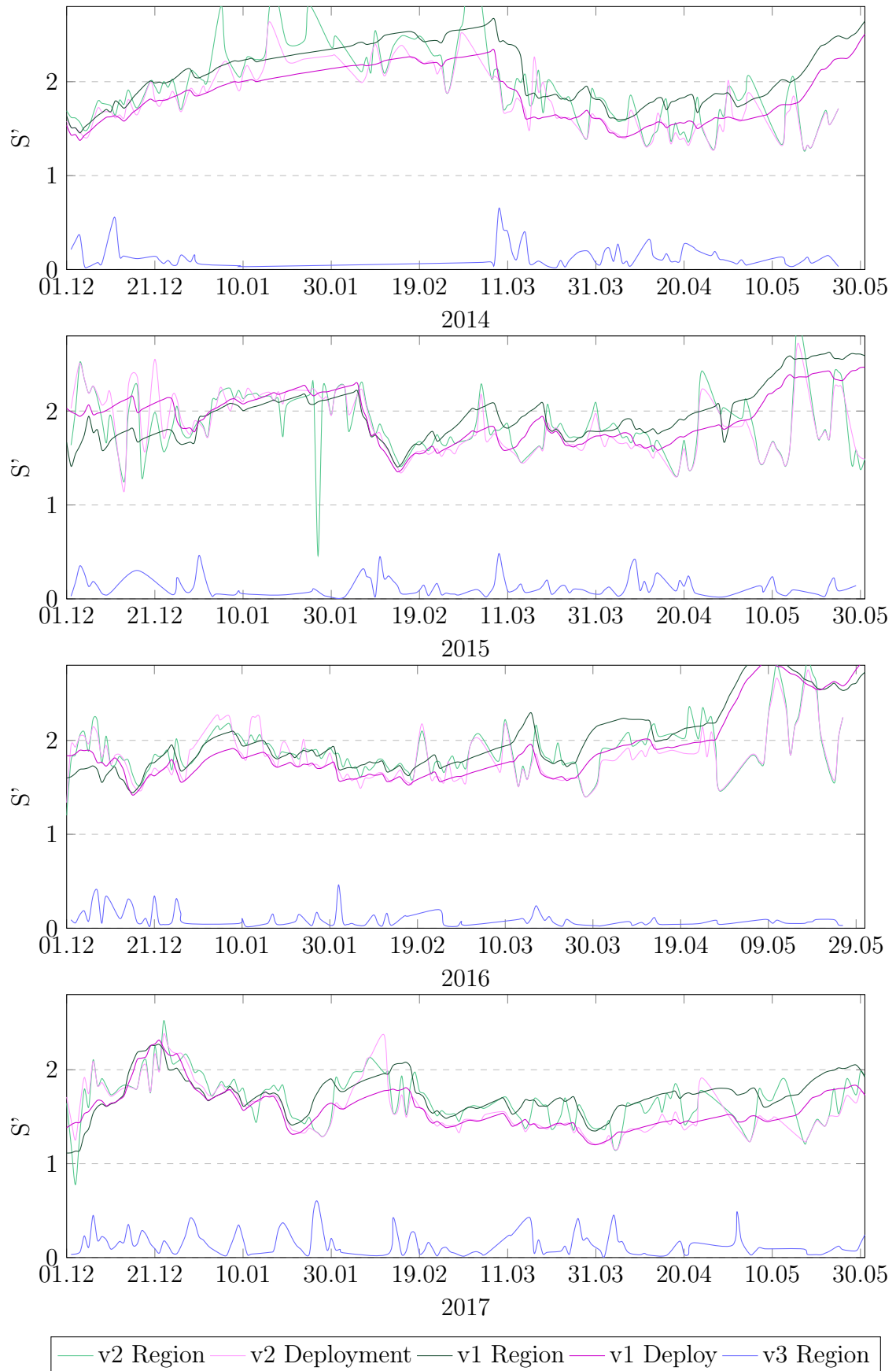


Figure 4.6 – Mean skier stability index for the four winter seasons in Lyngen.

When calculating S' , each grid point is calculated before averaging over the area. Figure 4.7 shows the distribution of S' v2 within the region of Voss in winter season 2014, before averaging. The red line marks the median, box represents the 25th and 75th percentile, and outliers are marked as points outside. These are points that are outside approximately 99.3 % coverage. Days with observed avalanche activity are marked in orange, while others are in blue. The smaller the 25th and 75th percentile box, the more agreement among all the grids in the region. If there is a big spread, it possible to have very unstable conditions in parts of the region, at the same time as there will be very stable conditions in other parts. There are no clear trends in S' for days with observed avalanche activity compared to days with no observed avalanche activity.

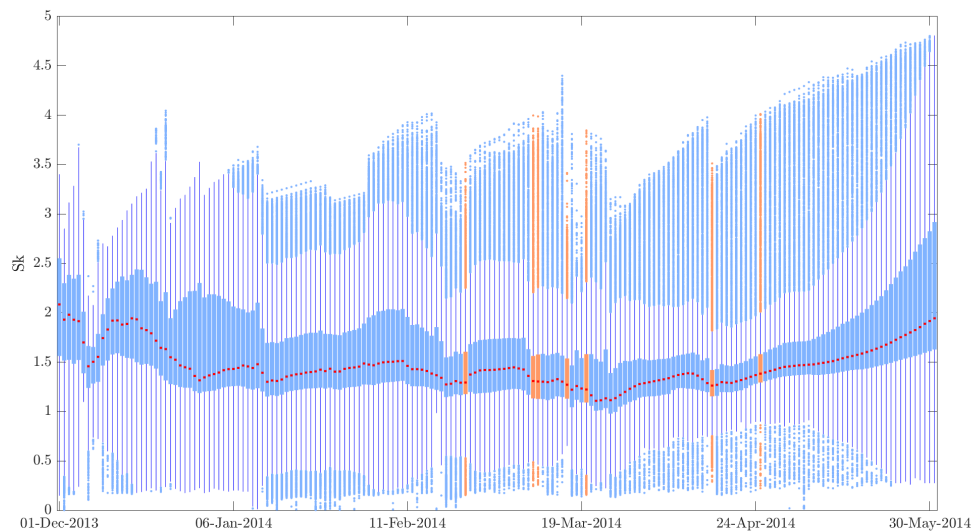


Figure 4.7 – Distribution of skier stability index over the winter season. Orange colored are days with observed avalanches. Red line marks the median, while the box represents the 25th and 75th percentile. Lines go to max and min, with outliers marked with point outside.

The lack of a complete avalanche history record can cause high bias when comparing dates of no registered avalanche activity with dates with registered avalanches. In this next part we will move on to examining the days with observed avalanche activity. Figure 4.8 shows an example of the spatial distribution of S' (v2 full region) in Voss (16th March 2014). This is one of several days with observed avalanches activity in the region (see Figure 3.1). S' has been calculated for all days with registered observed avalanches. Red color indicates less stable S' , while blue color indicate more stable conditions. Figure 4.8 has a generally low S' , with a median value of approximately 1.1. A way of investigating S' is to choose limits that give an indication of the stability

in the snow pack.

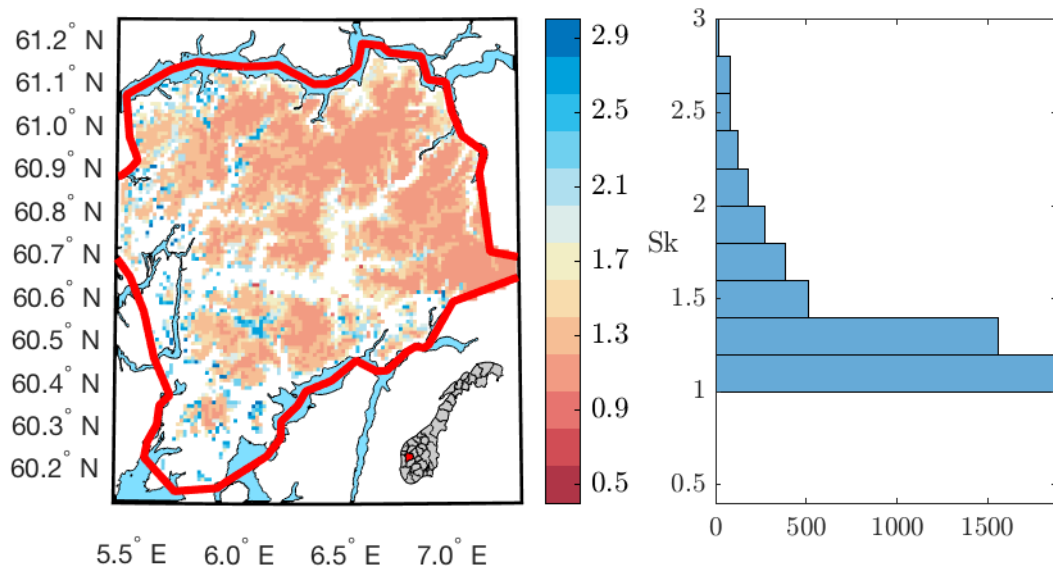


Figure 4.8 – Skier stability index in the region of Voss 16th March 2014, with distribution of Skier stability shown in panel on the right.

To check the success rate and if S' caught the instabilities, success limits have been defined. Following the success rates by Föhn (1987), 'success' is defined as S' less than or equal to 1 ($S' \leq 1$), 'semi-success' is when S' have the value between 1 and 1.5 ($1 < S' \leq 1.5$), and lastly 'misses' are all values above 1.5 ($S' > 1.5$). Complete overview of the success rate for the 21 A-regions can be seen in Figure 4.9 (v2), 4.10 (v1) and 4.11 (v3). Success is represented in green, semi-success in yellow and misses in red. There is great variation in how well S' performed in the different regions. Lowest success rate is in Vest Finnmark, and the northern regions, while higher success in west coast regions (e.g. Voss and Hardanger). A clear difference can be seen for v3 compared to the others. The high success rates can be related to the overall low stability estimated in v3.

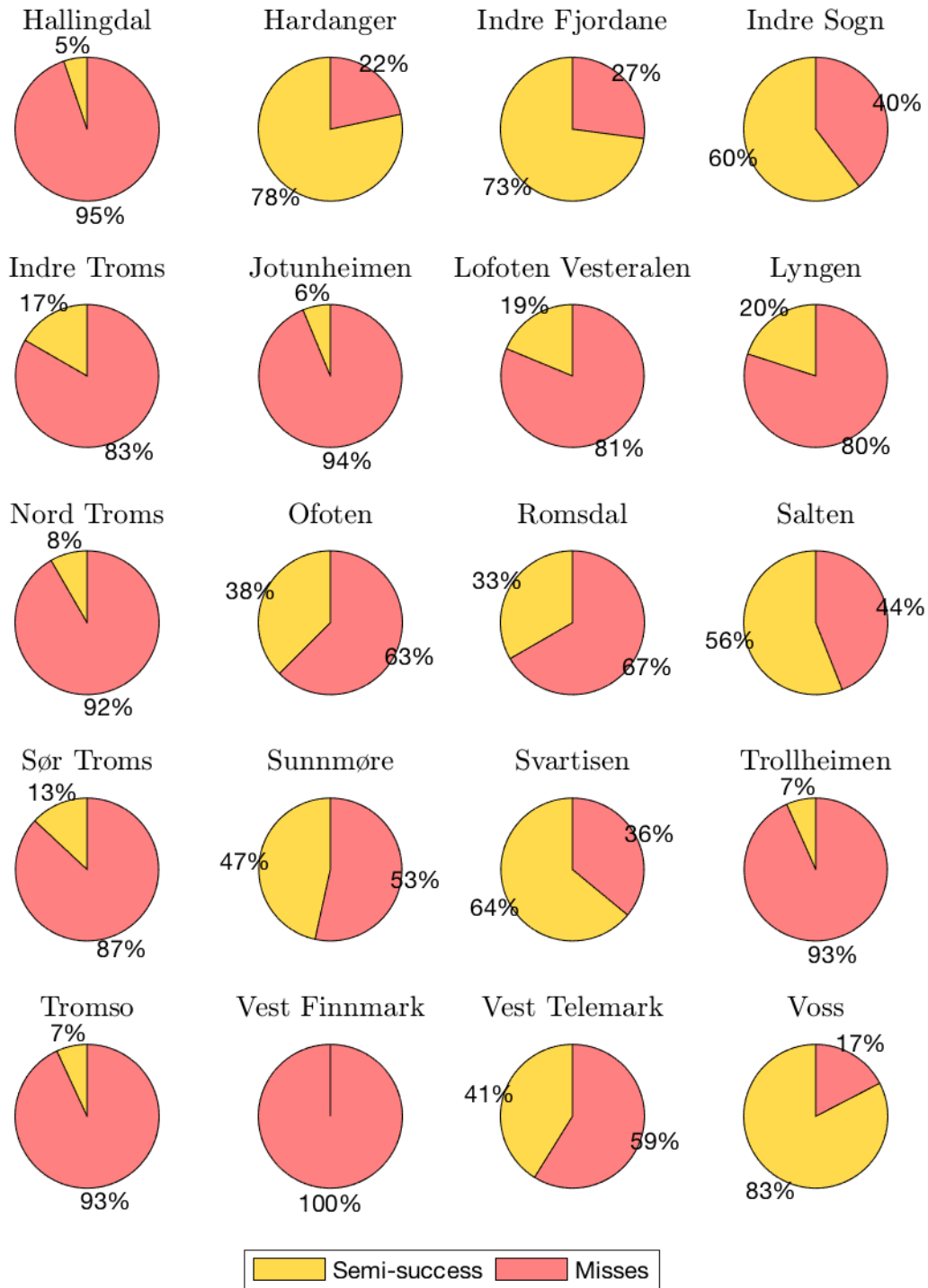


Figure 4.9 – Success rate for skier stability index(v2) full region, calculated for days with observed avalanche in A-regions. Nordiensiold no data. No attributes of success ($S' \leq 1$), semi-success can be seen in green($1 < S' \leq 1.5$) and misses ($S' > 1.5$) in red.

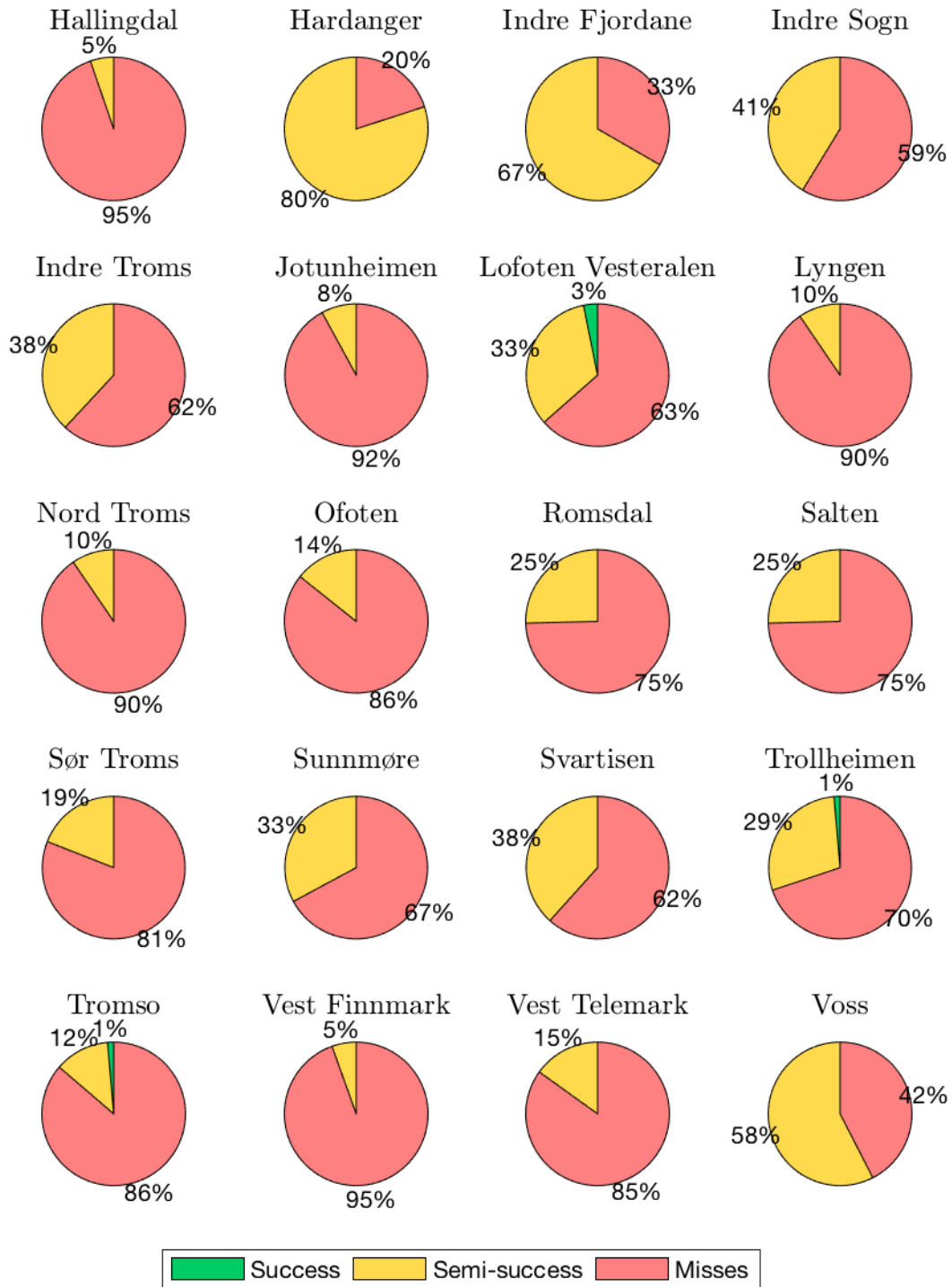


Figure 4.10 – Success rate for skier stability index (v1) full region, calculated for days with observed avalanche in A-regions. Nordienskiold no data. Attributes of success ($S' \leq 1$), semi-success can be seen in green ($1 < S' \leq 1.5$) and misses ($S' > 1.5$) in red.

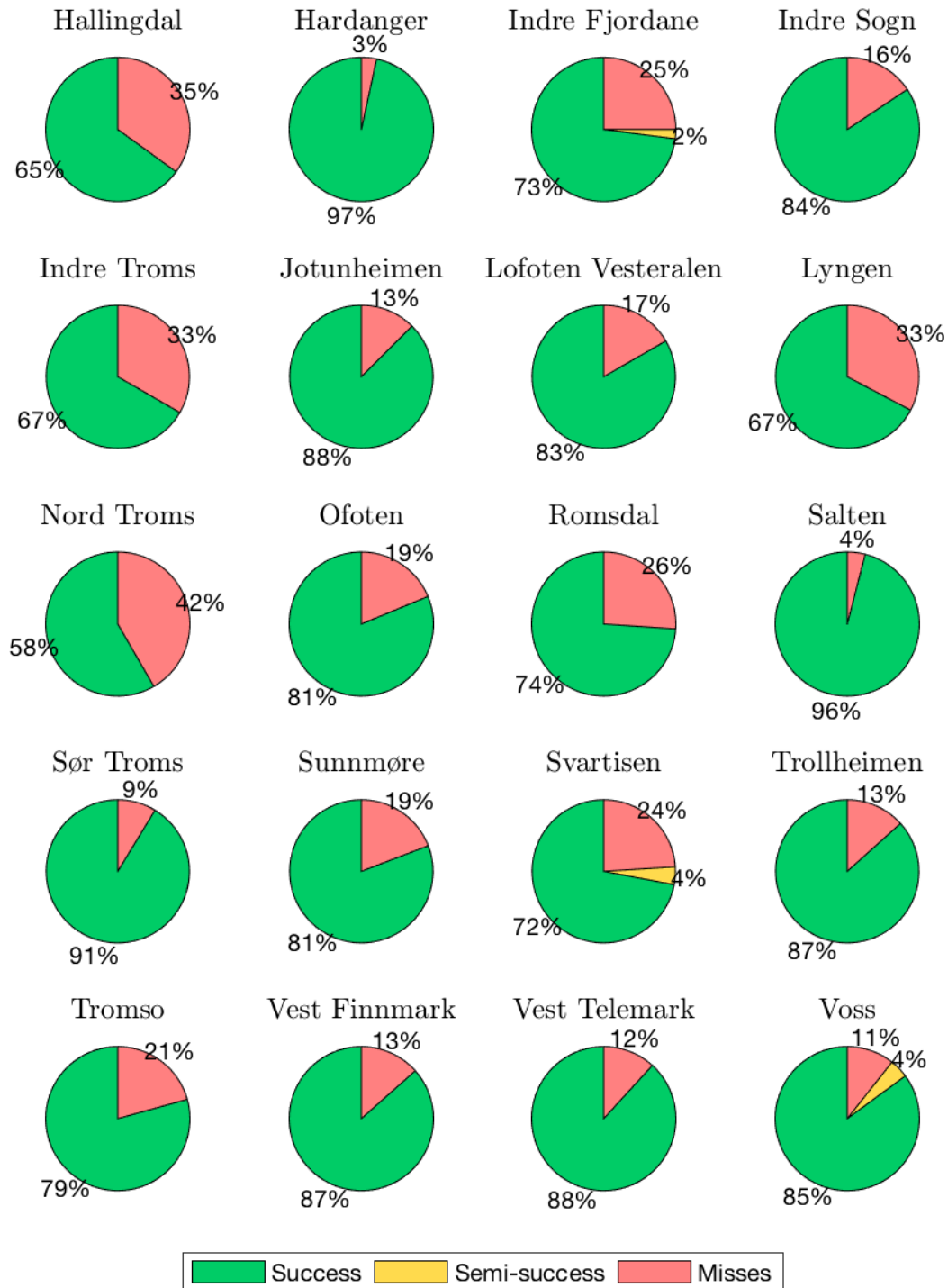


Figure 4.11 – Success rate for skier stability index (v3) full region, calculated for days with observed avalanche in A-regions. Nordiendskiold no data. Attributes of success ($S' \leq 1$), semi-success can be seen in green ($1 < S' \leq 1.5$) and misses ($S' > 1.5$) in red.

Looking even closer at the points with avalanche activity, by picking out the coordinates of observed avalanche, adding 0.2 rad (approximately 6 km diameter) around the point, and calculating S' for v2, full region. The results of this in Voss and Lyngen, winter season 2014 is shown in Figure 4.12 and 4.13, respectively. Red colors indicate more unstable conditions, while blue colors represent stable S' . As for the region data, the success rate for S' around the point has been calculated. Using the same limits as earlier; success ($S' \leq 1$), semi-success ($1 < S' \leq 1.5$), and misses ($S' > 1.5$). The results can be seen in Figure 4.14(v2) and 4.15(v1). Success is represented in green, semi-success in yellow and misses in red.

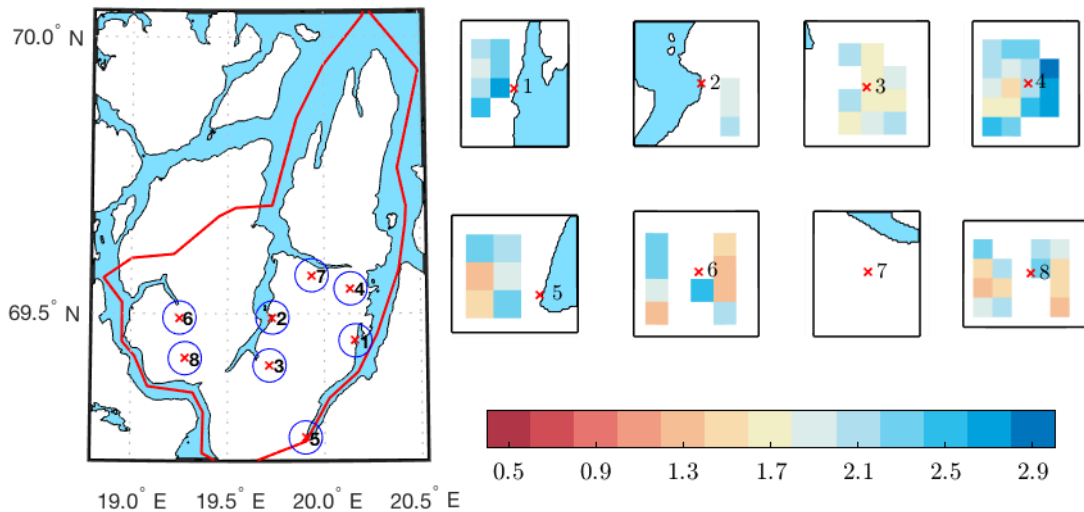


Figure 4.12 – Skier stability index, v2, for point of observed avalanches. Left panel: position of all observed avalanches in region of Lyngen winter season 2014, with a circle of rad= 0.2 around. Right panels: Skier stability index at day of observed avalanche, around the point of interest given from left panel.

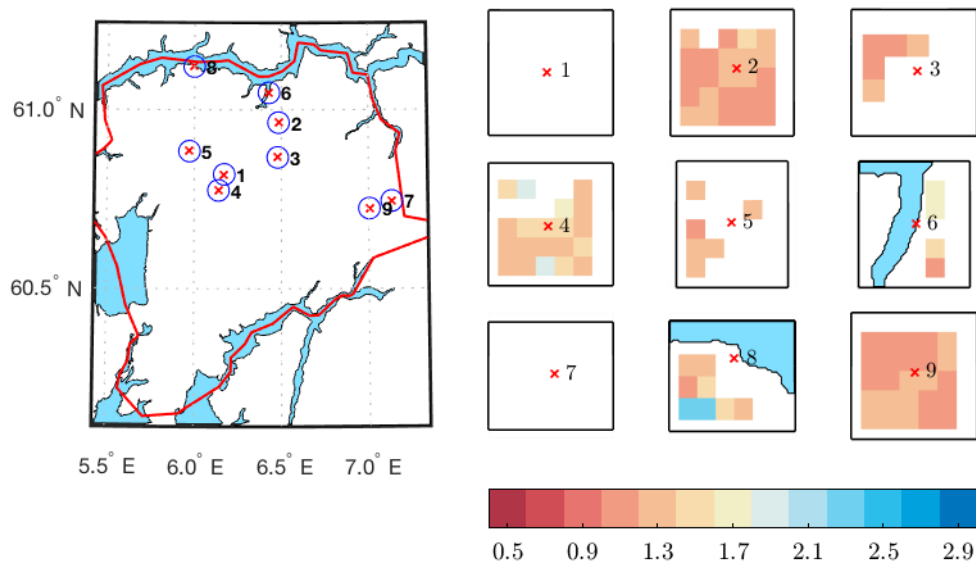


Figure 4.13 – Skier stability index, v_2 , for point of observed avalanches. Left panel: position of all observed avalanches in region of Voss winter season 2014, with a circle of $\text{rad} = 0.2$ around. Right panels: Skier stability index at day of observed avalanche, around the point of interest given from left panel.

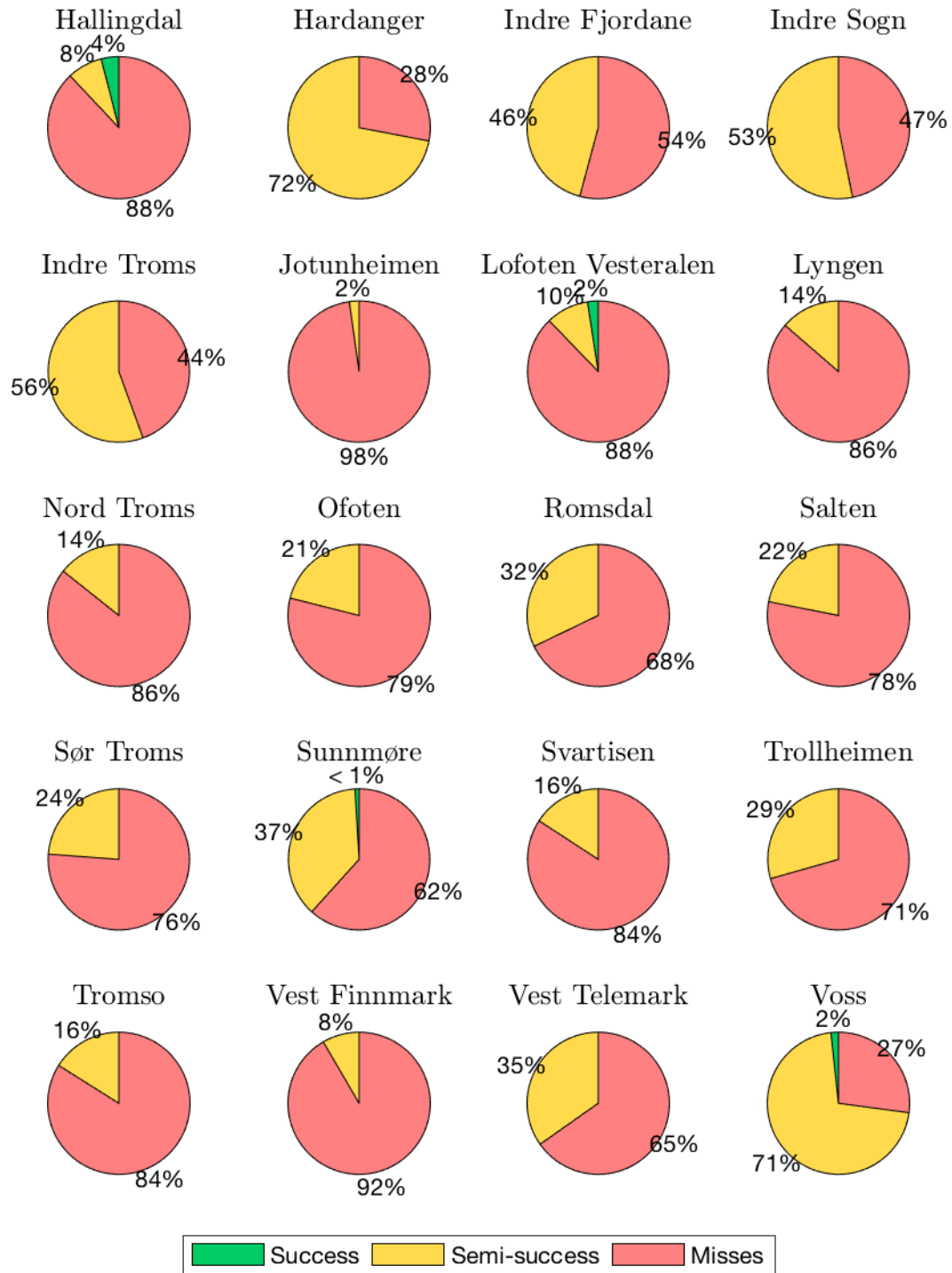


Figure 4.14 – Success rate for skier stability index, v_2 in point, calculated for days with observed avalanche in A-regions. Nordienskiold has no data. Success ($S' \leq 1$), semi-success can be seen in green ($1 < S' \leq 1.5$) and misses ($S' > 1.5$) in red.

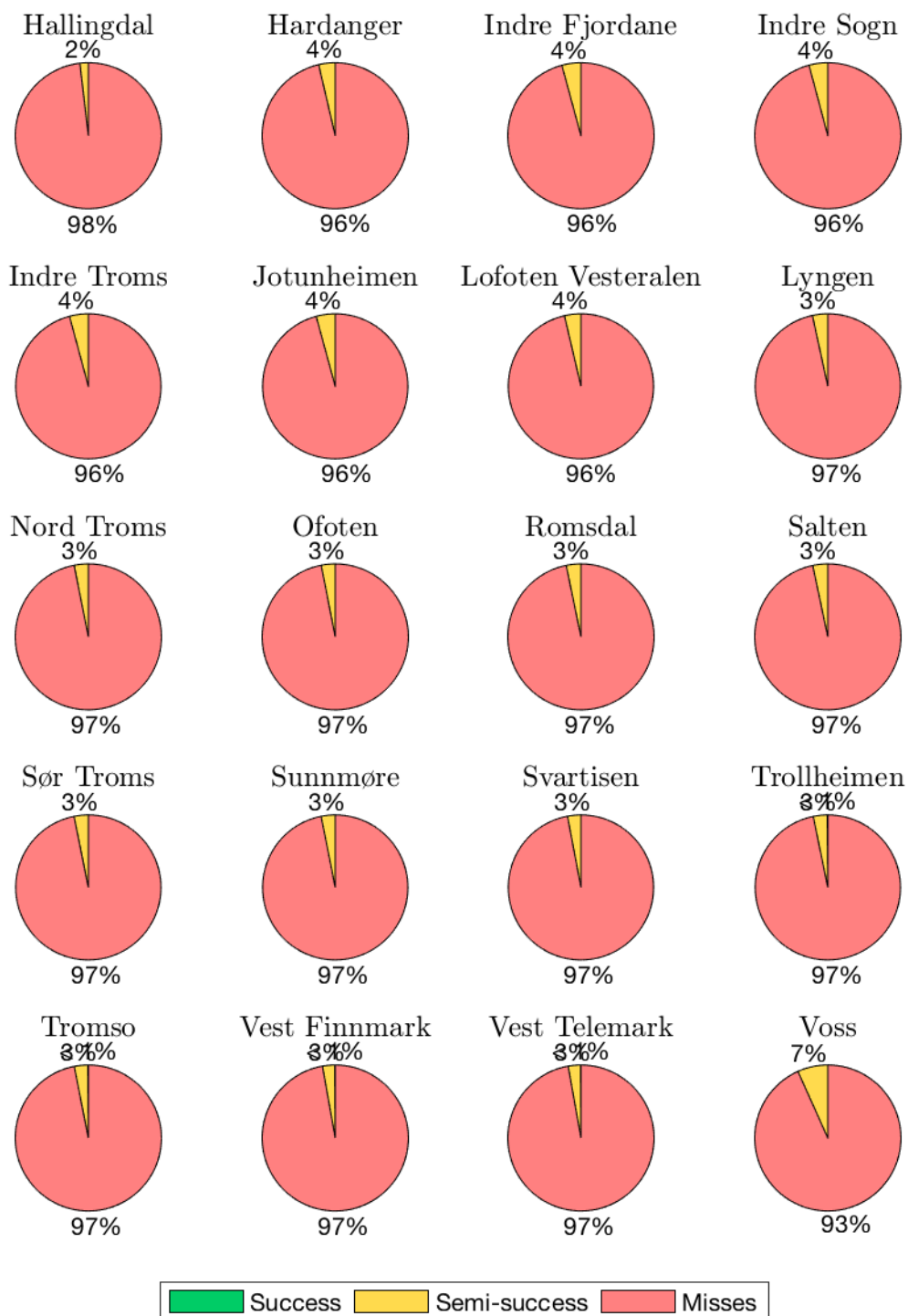


Figure 4.15 – Success rate for skier stability index, v_1 in point, calculated for days with observed avalanche in A-regions. Nordenskiöld has no data. Success ($S' \leq 1$), semi-success can be seen in green ($1 < S' \leq 1.5$) and misses ($S' > 1.5$) in red.

5 | Discussion

Skier stability index (S') is an index that tells us about the stability in a snowpack. By extending S to large scale, and using modeled snow data and weather forecast I have examined if it can be used as an addition to the current avalanche forecast in Norway. The success rate of S' on days with observed avalanches have been investigated. Though stronger in some regions, the success rate of S' on days with observed avalanches gives no clear indication of instabilities.

In this chapter I will systematically go through results, and discuss the findings and the meaning of these (Section 5.1). Some main questions that will be answered in this chapter are; Is the surface hoar growth realistic? How do the three versions of skier stability index compare to each other? What is the difference in S' between the grids; full region, deployment area vs point of avalanche? After, I will discuss some of the limitations that may have influenced the results (Section 5.2).

5.1 Interpretation of results

5.1.1 Surface hoar growth

In estimating the surface hoar growth, there are several simplifications made that can affect the results. One of these is the assumption that the created surface hoar layer stretches over the whole region. In nature this is very unlikely, surface hoar growth is dependent on that there is limited wind and radiation. In the mountain range you will have air flow and near surfaces turbulence that will affect the growth. It is common that surface hoar is created in "pockets" which are more sheltered. In the first months of the forecasting period incoming solar radiation is low, or non-existing in parts of Norway. This allows surface hoar to grow throughout the day. Further out in the season the days become longer and solar radiation plays a larger part in creating local variances of surface hoar growth.

Skier stability index (S') is not influenced by the surface hoar size, it only recognize a new surface hoar layer has been created. In Section 2.3.2 we saw that the size of a buried surface hoar layer can influence the instability.

5.1.2 V1 vs V2 vs V3

Evaluating the three versions of S' , introduced in Table 3.6, by comparing timelines and the score in success rates. The timelines, Figure 4.12 and 4.13, shows the difference between v1, v2 and v3 for the four forecasting seasons in Voss and Lyngen. As mentioned in Section 4.3, v3 has all over much lower scores than the two other versions. In both figures v3 has, for the most part, values below 1. This leads to the high success rates ($S' \leq 1$) on days with observed avalanches, with a mean success rate of approximately 80 %. The low values for all days would also lead to many false positives if the success rate for non-avalanche days had been investigated. Why does v3 have such lower values than the two other versions? The snow depth is much smaller in v3, as the layer only represents the accumulated snow depth from the last surface hoar layer. We saw in Figure 4.1 that shallower snow depths are destabilizing. Values of < 1 for whole region, every day, is very unrealistic. This implies that the snowpack is constantly in danger of sliding out, in all parts of the region. We saw in the previous section, Section 5.1.1, that a factor that might influence the results is the assumption of a constant surface hoar layer in the whole region.

V2 and v1 follows a more similar path, with v2 fluctuating more than v1. By comparing the two versions success rate for the full region, we can easier see how the two perform (Figure 4.9 and 4.10). V2 has no mean success rate, as there were no days with observed avalanches and skier stability index below one ($S' \leq 1$). The mean semi-success rate ($1 < S' \leq 1.5$) is approximately 34 %. V1 has a mean success rate $< 1\%$, and a mean semi-success rate of approximately 28 %.

Comparing also the success rate by the two versions calculated inside area surrounding avalanche observations, Figure 4.14 and 4.15. Here v2 has a mean success rate < 1 , and a mean semi-success rate of 29 %. V1 has an equal mean success ($< 1\%$), and a mean semi-success rate of 3 %. In both cases v2 has a higher success of catching instabilities than v1.

5.1.3 Deployment areas vs Region vs Point of avalanche

How do the three different grids compare to each other? As for the comparison of the three version of S' , we will first use the timelines plotted for the four forecasting seasons in Voss and Lyngen, Figure 4.12 and 4.13, to investigate the difference between full region and deployment area. Region is given in light and dark green, while deployment is in light and dark pink, where light colors represent v2 and darker colors represent v1. In both regions there are very little difference between full region and deployment area. In Voss, the deployment area S' is a little more stable than full region, while in

Lyngen we see the opposite. The small variation between the two grid versions is why v3 and success rates are only estimated for full region data.

Comparing full region with calculations of S' in point of interest to see if there will be change when only including grids close to the observed avalanche. The circles around the point in which S' is calculated is approximately 6 km in diameter. Considering the high variations both in terrain and weather conditions in mountains, 6 km is still “low” spatial resolution in catching avalanche conditions. The full region has higher semi-success rates in both v1 and v2. 34 % and 28 % in full region, against 29 % and 3 % in point of interest.

5.2 Limitations

As we have now seen, the Skier stability index (S') are showing low success rates in all versions, except v3 which is underestimating S' at all times. I will now look closer at some of the limitations that might have affected the calculations, causing the low success rates. First, I will look into some aspects of the calculations of S' , before discussing limitations set by the datasets used.

5.2.1 Skier stability index

There are some important limitations of S' to take into account when analyzing the results. One of the most important factors is how S' , in this case, have been limited to only represent buried surface hoar layers. As mentioned in Section 2.3.2 and Appendix A there are several non-persistent NP and persistent layers (P). Buried surface hoar layer is the persistent layers which has taken most lives in skier triggered slab avalanches (Tremper, 2008), making this a natural choice of layer to investigate closer. At the same time, this means we will not catch the presence of, e.g., depth hoar layers, which is a common layer in continental climates, and intermountain climates (McClung, 2006). This is a more frequent layer in the Northern parts of Norway than further south. In the North there is often low temperatures, giving a strong temperature gradient in the snowpack, which is favorable conditions for depth hoar formation.

5.2.2 Avalanche history record

One of the main limitations for validation of the Skier stability index (S') is the low number of avalanche observations. For the four seasons there were in total 2202 avalanche observations recorded. The present winter season has just come to an end. During this season there has been a large campaign by varsom.no, to make people aware of

the possibility to register your avalanche observations in regObs. In the last year there were over 4000 observations registered in regObs (Varsom.no, 2018b). This gives a clear indication that the prior dataset of observations are lacking. With the low number of avalanches in each region each year, see examples in Figure 4.4 and 4.7, the possibility of checking days without observed avalanches is not possible.

The last year, newer technology has enabled the possibility of using radar and satellite imagery to make avalanche observations. These new observations, as well as the increase in regObs registrations, will come to great value for future research in the field of snow avalanche in Norway.

The limitations set by the avalanche history record is why the main focus of this thesis has been controlling days with observed avalanche activity. With newer database it would be interesting to investigate the success rates for days without observed avalanche activity.

As for the validations done when calculating the success rates for S' on days with observed avalanches, most days we do not know what type of avalanche that is released. Table 3.3 and Figure 3.1 gives the attributes of avalanche types and the distribution of the 2202 avalanche observations. The descriptions of the attributes lack information on what kind of weak layer is present in the release of slab avalanches. There are also 34 % that is attributed with unspecified avalanche (1 % point release unspecified, 4 % slab unspecified and 29 % unspecified). Leaving room for big variations in type of avalanche that is observed.

5.2.3 Spatial and temporal resolution of the data

The two data sets used for variables in the calculations are the NVE data described in Section 3.1.1 and MEPS described in Section 3.1.2. NVE has a spatial resolution of 1 km, while MEPS has a spatial resolution of 2.5 km.

The main reason for using the NVE data set is to stay as close to the present avalanche forecast as possible. Using a 1 km resolution grid when working with snow-cover is still a "coarse" resolution, as snow has large spatial variability (Section 2.1.2) The hope is that from the grid, the mean of spatial variation will be represented by the dataset. For an avalanche to release, there only needs to be a "hotspot" of weaker snow, to make the conditions unstable enough for an avalanche. This will not be caught by the 1 km resolution NVE data set.

The NVE data set comes in 24 h temporal resolution. In snow avalanches the loading rate of snow can be crucial for the stability. Having a large load of new snow fall in a shorter period of time causes greater instabilities than loading slowly. In the 24 h resolution, the time frame is too large to get any information in how fast the loading

is. The load in this thesis has been evaluated as static - independent of time. Using a higher time resolution data set would allow to introduce dynamic loads from the snow. Loading dependent on the snow rate.

The MEPS data set is only used in calculating the surface hoar, the spatial limitations of this have already been discussed in Section 5.1.1. In this thesis the variables have been averaged on a daily basis, to be able to compare with the 24 h time resolution of the NVE data set. Surface hoar formation is most common on clear winter night (Section 3.3.3), if working further with exploring the skier stability index, exploring the effects of only averaging night vs day data could be an improvement to the current calculations.

6 | Summary and outlook

In this section I will give a concise summary to the investigation of Skier stability index (S') as an addition to the avalanche forecast in Norway.

6.1 Summary

At present point the Skier stability index (S') will not give a great contribution to the avalanche forecast. With low success rates, and highly varying results for each region, it is hard to see a clear indication of instabilities from the values estimated.

Of the three versions of S' calculated, highest success rates on days with avalanche observed is v3; S' with implemented surface hoar layers. The problem with v3, is it also gives false positive on days where there are no observed avalanches. On second place is v2, which assumes one homogeneous layer of the whole snowpack. Average semi-success rates ($1 < S' \leq 1.5$) of 34 % and 29 % for the full region grid and around points of observed avalanche, respectively.

Three grid estimates have also been compared; full region, deployment area and point of avalanche. There were small differences between the full region and deployment area estimates. Because of these small differences grid point of avalanche was only compared with full region. The full region had higher semi-success rates in both v1 and v2 than point of avalanche data. 34 % and 28 % in the full region, against 29 % and 3 % in the point of avalanche.

Limitations of the calculations and data sets were briefly discussed in Chapter 5. One main issue to highlight is the limited avalanche observations data set. The lack of observations makes validation of the estimates harder to do. In the thesis it is only used days of avalanche observations to validate, not days where there are no observations, with the exception of v3. Which showed $S' \leq 1$ for all days in the forecasting season. We can then assume that the v3 showed unstable conditions on days with no avalanche activity.

6.2 Recommendation for further work

A further study into the Skier stability index (S') is still very interesting, even though this study shows high uncertainty. Some aspects to consider to improving S' has been mentioned in Chapter 5. Another aspect that would be interesting to investigate further is using S' to give a danger level for avalanche. When setting the danger level for avalanches, (see Figure 2.10) the size of the avalanche, as well as on how big part of the region the danger is valid for, are used. Using the distribution of the S' in a region, threshold values could be investigated to see if they could contribute to deciding the avalanche danger level. Larger areas of low stability, gives higher danger level.

As noted in Section 5.2.2, there has been an increase in registration of avalanche activities by public, following a large campaign by Varsom.no to get more people to use regObs. With improved datasets of observed avalanches, from public and from the advancing use of satellite and radar, the foundation for validation of research on snow avalanches have increased. It will be interesting to follow the development in avalanche research in the time to come.

7 | Bibliography

- Armstrong, R. L. and Brun, E. (2008). *Snow and Climate: Physical Processes, Surface Energy Exchange and Modeling*. Cambridge University Press.
- Clelland, M. and O'bannon, A. (2012). *Allen & Mike's avalanche book: A guide to staying safe in avalanche terrain*. Rowman & Littlefield.
- Conway, H. and Abrahamson, J. (1984). Snow stability index. *Journal of Glaciology*, 30(106):321–327.
- Engeset, R. V. (2016). Hvordan lages nedbør, lufttemperatur og snødata på seNorge. Technical report, Norges Vassdrags- og Energidirektorat.
- Fierz, C., Armstrong, R., Durand, Y., Etchevers, P., Greene, E., McClung, D., Nishimura, K., Satyawali, P., and Sokratov, S. (2009). The international classification for seasonal snow on the ground. *IHP-VII Technical Documents in Hydrology*, 83(1):90.
- Föhn, P. M. B. (1987). The stability index and various triggering mechanisms. *IAHS Publ.*, 162(162):195–214.
- Hachikubo, A. (2000). Roughness effect on vapor transfer for surface hoar growth. *International Snow Science Workshop*, pages 128–134.
- Hisdal, H. (2017). Evaluering av snø-og jordskredvarslingen. *Norges vassdrags- og energidirektorat*, 30.
- Horton, S., Bellaire, S., and Jamieson, B. (2014). Modelling the formation of surface hoar layers and tracking post-burial changes for avalanche forecasting. *Cold Regions Science and Technology*, 97:81–89.
- Jamieson, B. and Johnston, C. D. (2001). Evaluation of the shear frame test for weak snowpack layers. *Annals of Glaciology*, 32:59–69.
- Jamieson, J. B. (1995). *Avalanche prediction for persistent snow slabs*. PhD thesis, University of Calgary.

-
- Landry, C., Birkeland, K., Hansen, K., Borkowski, J., Brown, R., and Aspinnall, R. (2004). Variations in snow strength and stability on uniform slopes. *Cold Regions Science and Technology*, 39(2-3):205–218.
- Lussana, C., Saloranta, T., Skaugen, T., Magnusson, J., Einar Tveito, O., and Andersen, J. (2018a). SeNorge2 daily precipitation, an observational gridded dataset over Norway from 1957 to the present day. *Earth System Science Data*, 10(1):235–249.
- Lussana, C., Tveito, O. E., and Uboldi, F. (2018b). Three-dimensional spatial interpolation of 2 m temperature over Norway. *Quarterly Journal of the Royal Meteorological Society*, 144(711):344–364.
- McClung, D. (2006). *The Avalanche Handbook*. The Mountaineers books, 3 edition.
- Mueller, M., Homleid, M., Ivarsson, K.-I., Koltzow, M. A. O., Lindskog, M., Midtbo, K. H., Andrae, U., Aspeli, T., Berggren, L., Bjorge, D., Dahlgren, P., Kristiansen, J., Randriamampianina, R., Ridal, M., and Vignes, O. (2017). AROME-MetCoOp: A Nordic Convective-Scale Operational Weather Prediction Model. *Weather and Forecasting*, 32(2):609–627.
- Müller, K., Kosberg, S., Barfod, E., Rustad, B. K., and Landrø, M. (2013). Snøskredvarslingen - Evaluering av vinteren 2013. Technical report, Norges Vassdrags- og Energidirektorat.
- Norem, H. (2011). *Veger og snøskred*. Vegdirektoratet.
- Norges Vann- og Energiressurser (2017). Skredhendelser. <https://www.nve.no/flaum-og-skred/kartlegging/skred-og-flaumhendinger/skredhendelser/>. [Online; accessed 01-04-2017].
- Peereboom, I. (2015). Produktark : Snøskred - aktsomhet. *Norges Vassdrags- og Energidirektorat*.
- Perla, R., Beck, T. M., and Cheng, T. T. (1982). The shear strength index of alpine snow. *Cold Regions Science and Technology*, 6(1):11–20.
- Roch, A. (1966a). Les déclenchements d’avalanches. *Union de Géodésie et Géophysique Internationale. Association Internationale d’Hydrologie Scientifique. Commission pour la Neige et la Glace. Division Neige Saisonnière et Avalanches. Symposium international sur les aspects scientifiques des avalanches de*, pages 182–183.
- Roch, A. (1966b). Les variations de la résistance de la neige. *Proceedings of the International Symposium of Scientific Aspects of Snow and Ice Avalanches, Gentbrugge, Belgium, International Association of Hydrological Sciences*, pages 182–195.
- Schweizer, J. and Jamieson, J. B. (2001). Snow cover properties for skier triggering of avalanches. *Cold Regions Science and Technology*, 33(2-3):207–221.

- Schweizer, J. and Jamieson, J. B. (2004). Snow stability measurements. *Proceedings of the International Seminar on Snow and Avalanche Test Sites, Grenoble, France*, pages 317–331.
- Stull, R. B. (1988). *An Introduction to Boundary Layer Meteorology*, volume 13. Springer Science & Business Media.
- Thomson, R. E. and Emery, W. J. (2014). *Data Analysis Methods in Physical Oceanography*. Elsevier, third edition.
- Tremper, B. (2008). *Staying alive in avalanche terrain*. The Mountaineers Books.
- Varsom.no (2017). Slik utarbeides snøskredvarselet. <http://www.varsom.no/nytt/nyheter-snoskred/slik-utarbeides-snoskredvarselet/>. [Online; accessed 01-05-2018].
- Varsom.no (2018a). Avalanche Bulletin. <http://www.varsom.no/en/avalanche-bulletins/>. [Online; accessed 10-04-2018].
- Varsom.no (2018b). Økning i antall frivillige observasjoner på regObs. <http://www.varsom.no/nytt/nyheter-snoskred/okning-i-antall-frivillige-observasjoner-pa-regobs/>. [Online; accessed 20-05-2018].
- Varsom.no (2018c). Snøskredulykker- og hendelser. <http://www.varsom.no/ulykker/snoskredulykker-og-hendelser/>. [Online; accessed 01-05-2018].
- Young, H. D., Freedman, R. A., Ford, A. L., and Sears, F. W. (2004). *Sears and Zemansky's university physics : with modern physics*. Pearson Addison Wesley, San Francisco, 13 edition.

A | Weak layers and interfaces in the snowpack

Table A.1 – Weak layers and interfaces in the snowpack

Name	Description	P/NP Persistence	
Weak layers in the snow pack			
Unchosive new snow	Low-density snow or density inversions in the new snow - relatively more cohesive snow sliding on relatively less cohesive snow.	NP	Stabilises within hours to days depending on temperature
Graupel	Common layer in maritime climate. Often slides and gathers in less steep terrain.	NP	Stabilizes about 1-2 days after deposition.
Weak interfaces/crusts			
Sun crust	Heat from sun melts the snow surface, which then refreezes. Sometimes form a hard bed surface for future avalanche to run upon. Rough texture compared to rain crust.	NP/P	Stabilizes fairly quickly after a storm.
Melt-freeze crust	Undergoes repeated cycles of melting and freezing, which rounds the snow grains and they grow in size with each repeated cycle of melting and freezing.		
Rain crust	More smooth and slippery than sun crust. Created by rain that freezes.	NP/P	Persist for several days, sometimes several storms.
Weak layers within the old snow			

Continued on next page

Table A.1 – continued from previous page

Name	Description	P/NP Persistence	
Faceted snow	Faceted snow is created by large temperature gradients in the snowpack. Critical temperature is 1°Cpr 10 cm. Often referred to as "sugarsnow" in Norway, no bindings between the crystals.	P	
Depth hoar	Faceted snow near the ground. Ground is almost always warm, except permafrost areas or in areas with a thin snow cover combined with very cold temperatures. Stronger in compression than in shear, it can also fail in a catastrophic collapse of the layer. Fracture propagate long distances and around corners.	P	Extremely persistent, several days to several weeks, depending on temperature. Larger the grain, the more persistent.
Near surface faceted snow	Similar to depth hoar, and faceted snow.	P	Very persistent
Surface hoar	Created with clear skies, no direct sunshine, calm or light winds, and humid air. Form "feather" like crystals on the surface of the snow	P	Extremely persistent when buried. One week to months depending on temperature. Especially persistent and dangerous when on top of a firm ice crust.